	Form Approved OMB NO. 0704-0188

1. AGENCY USE ONLY (Leave Blank)	2. REPORT DATE	3. REPORT TYPE AND DATES COVERED
	03-07-2008	Final report, 12.07.06-12.07.07

4. TITLE AND SUBTITLE	5. FUNDING NUMBERS
Molecular Design of Sulfonated Triblock Copolymer Permselective Membranes	W911NF-07-1-0048
6. AUTHOR(S) Aleksey Vishnyakov and Alexander V. Neimark	
7. PERFORMING ORGANIZATION NAME(S) AND ADDRESS(ES) Department of Chemical and Biochemical Engineering Rutgers, the State University of New Jersey	8. PERFORMING ORGANIZATION REPORT NUMBER n/a
9. SPONSORING / MONITORING AGENCY NAME(S) AND ADDRESS(ES) U. S. Army Research Office P.O. Box 12211 Research Triangle Park, NC 27709-2211	10. SPONSORING / MONITORING AGENCY REPORT NUMBER 52305.1-CH

11. SUPPLEMENTARY NOTES

The views, opinions and/or findings contained in this report are those of the author(s) and should not be construed as an official Department of the Army position, policy or decision, unless so designated by other documentation.

12 a. DISTRIBUTION / AVAILABILITY STATEMENT	12 b. DISTRIBUTION CODE
Approved for public release; distribution unlimited.	

13. ABSTRACT (Maximum 200 words)

Search for novel polymeric electrolyte membranes (PEM) suitable as permselective diffusion barriers is one of the key problems in engineering new protective materials. The goal of the project was to get a better understanding of the physical and chemical factors governing sorption and permeability of phosphoorganic agents in PEM made of sulfonated triblock copolymers of styrene and lower olefins by means of multiscale molecular simulations. These materials are of special interest to the Army as low-cost substitutes of expensive Nafion-type membranes. Concentrating on sulfonated polystyrene containing block-copolymers, we developed a hierarchical multiscale methodology for computational studies of the membrane morphology at environmental conditions, and the membrane sorption and transport properties with respect to water and nerve gas simulant dimethylmethylphosphonate (DMMP). The methods developed include: a) quantum mechanical ab-initio calculations of specific interactions of DMMP and water with the membrane fragments, b) atomistic molecular dynamic simulations of membrane solvation in water-DPPM mixture with different counterions, c) large-scale molecular dynamic simulations of membrane segregation and mobilities of chemicals, and d) dissipative particle dynamics simulations of mesoscopic morphologies in solvated membranes of different composition. The molecular simulation studies were performed in concert with the experimental work at Natick Soldier RDEC, Natick, Ma

14. SUBJECT TERMS	15. NUMBER OF PAGES
protective materials, polymeric electrolyte membranes, phosphor-organic agents, DMMP, molecular simulation	38
	16. PRICE CODE

17. SECURITY CLASSIFICATION OR REPORT	18. SECURITY CLASSIFICATION ON THIS PAGE	19. SECURITY CLASSIFICATION OF ABSTRACT	20. LIMITATION OF ABSTRACT
UNCLASSIFIED	**UNCLASSIFIED**	**UNCLASSIFIED**	**UL**

NSN 7540-01-280-5500

Standard Form 298 (Rev.2-89)
Prescribed by ANSI Std. 239-18
298-102

Enclosure 1

Final Report (W911NF-07-1-0048)

Molecular Design of Sulfonated Triblock Copolymer Permselective Membranes

Aleksey Vishnyakov and Alexander V. Neimark*
Department of Chemical and Biochemical Engineering
Rutgers, the State University of New Jersey
98 Brett rd, Piscataway NJ 08854

Summary.

Search for novel polymeric electrolyte membranes (PEM) suitable as permselective diffusion barriers is one of the key problems in engineering new protective materials. These membranes must be impermeable to CWA and, at the same time, provide high water vapor permeability, small heat accumulation, and reduced weight. The goal of the project was to get a better understanding of the physical and chemical factors governing sorption and permeability of phosphoorganic agents in PEM made of sulfonated triblock copolymers of styrene and lower olefins by means of multiscale molecular simulations. These materials are of special interest to the Army as low-cost substitutes of expensive Nafion-type membranes. To enhance experimental studies, one needs to predict how the chemistry of PEM, its composition, and counterions would affect sorption and transport of ions and chemicals in solvated membranes Concentrating on sulfonated polystyrene containing block-copolymers, we developed a hierarchical multiscale methodology for computational studies of the membrane morphology at environmental conditions, and the membrane sorption and transport properties with respect to water and nerve gas simulant dimethylmethylphosphonate (DMMP). The methods developed include: a) quantum mechanical *ab-initio* calculations of specific interactions of DMMP and water with the membrane fragments, b) atomistic molecular dynamic simulations of membrane solvation in water-DPPM mixture with different counterions, c) large-scale molecular dynamic simulations of membrane segregation and mobilities of chemicals, and d) dissipative particle dynamics simulations of mesoscopic morphologies in solvated membranes of different composition. The results of simulations of triblock copolymers were compared with those of Nafion. The molecular simulation studies were performed in concert with the experimental work at Natick Soldier RDEC, Natick, Ma.

* Principal Investigator, aneimark@rutgers.edu

I. Introduction.

Search for novel polymeric electrolyte membranes (PEM) suitable as permselective diffusion barriers is one of the key problems in engineering new protective materials. These membranes must be impermeable to CWA and, at the same time, provide high water vapor permeability, small heat accumulation, and reduced weight. Current research focuses primarily on PEM, such as Nafion-type perfluorinated ionomers and sulfonated triblock copolymers of styrene and lower olefins, which may provide desired protective, comfort, and mechanical properties. In our earlier works, we studied molecular interactions of nerve gas simulant dimethylmethylphosphonate (DMMP) with Nafion. This project, which is a continuation of the project W911NF-04-1-0239, aimed at the development of the multiscale simulation methods for studies of PEM made of sulfonated triblock copolymers of styrene and lower olefins. These materials are of great interest to the Army as low-cost substitutes of expensive Nafion-type membranes. The goal of the project was to get a better understanding of the physical and chemical factors governing sorption and permeability of phosphoorganic agents in triblock copolymers by means of multiscale molecular simulations. These molecular simulation studies were performed in concert with the experimental work at Natick Soldier RDEC, Natick, Ma (Drs. Schneider and Rivin).

Engineering properties of PEM are determined by the membrane nanoscale morphology and chemical composition. Triblock copolymer PEM, as well as Nafion, possess a complex hierarchical structure. They are built of nanoscale blocks arranged in self-assembled mesoscopic structures. Depending on the system and environmental conditions, these self-assembled structures may have either regular symmetric or disordered morphologies. Sorption and transport properties of a self-assembled system depend not only on its chemical composition but also on its morphology. The hierarchical structure of PEM implies a hierarchy of modeling tools, which span many orders of magnitude of special and temporal scales (Figure 1). We apply a multiscale hierarchical approach, which involves different simulation methods at different length and time scale.

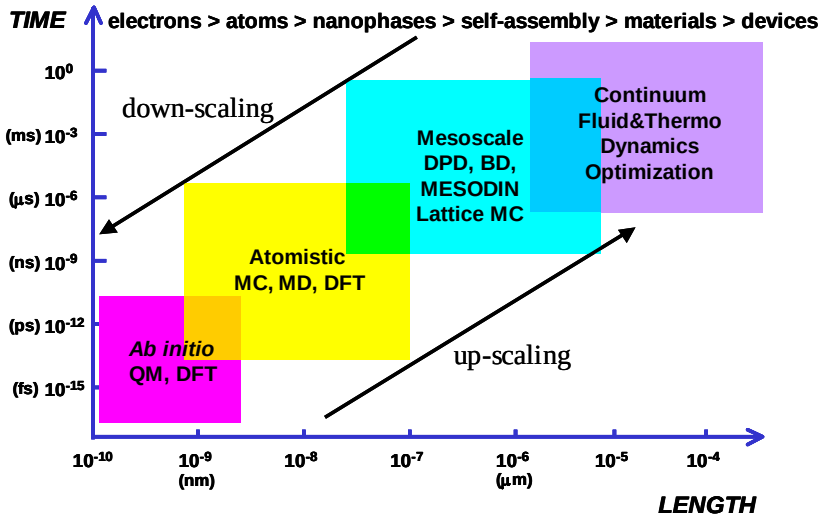

Figure 1. Typical length and time scales in multiscale simulation of functional nanomaterials.

This approach enables us to describe the macroscopic properties of PEM from *ab-initio* quantum mechanical calculations of electron density to atomistic molecular dynamics and Monte Carlo (MC) simulations to coarse-grained mesocsopic methods of dissipative particle dynamics (DPD). In so doing, the results of simulations on lower scale level serve as input parameters for simulations on upper scale level.

The polyelectrolytes considered in this work are shown in Figure 2, Kraton-type sulfonated block copolymers are studied in interaction with water and DMMP. Nafion-type perfluorinated polymers serve as the reference for comparative analyses.

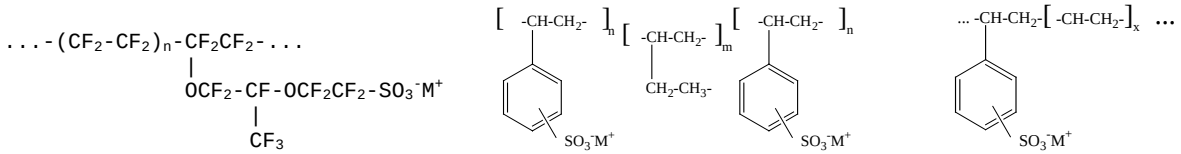

Figure 2. Chemical formulae on some of the candidate polyelectrolytes for protective membranes: Nafion (left), sulfonated polysterene–poly(buta-1-ene)–polysterene triblock copolymers (middle), pseudorandom styrene-ethylene copolymer (right) [1].

The strategy of hierarchical multiscale simulations is given schematically in Figure 3. Unique permselective properties of PEM are related to their complex nanostructure. In the presence of water and other polar solvents, these ionomers segregate into hydrophilic and hydrophobic subphases. In Nafion, the hydrophilic subphase is formed by water (and/or other hydrophilic solvent), hydrophilic sidechains, and counterions, while the hydrophobic subphase is formed by perfluorinated backbone. In block-copolymers, sulfonated blocks form the hydrophilic phase, and olefin blocks make the hydrophobic subphase.

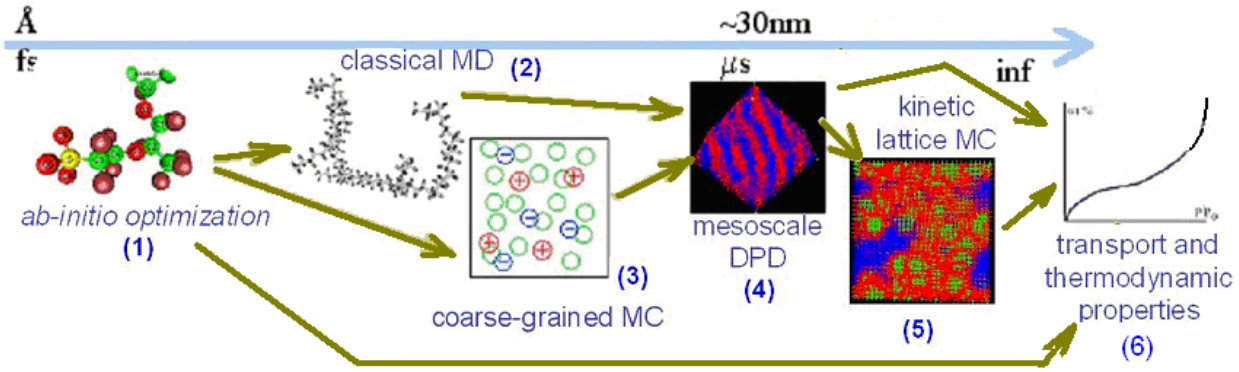

Figure 3: Multiscale computational scheme with the examples from Nafion and Kraton block copolymers simulations by the PI. The numbers correspond to the simulation methods employed in this project (1) Nafion side chain optimized by RHF method, (2) MD simulations of Nafion, (3): coarse-grained electrolyte solution; (4) DPD modeling of segregation in hydrated Kraton; (5) random walk lattice MC modeling of chemicals diffusion in segregated PEM membranes (6) thermodynamic modeling of interactions of chemicals with fragments of PEM using COSMO-RS model based on the results of ab-initio optimization.

The overall strategy of the multiscale approach is reflected in the structure of this report. A brief literature review is given in Section II, which justifies the use of the multiscale approach. First, we have either to adopt from the literature or to create the forcefields (interaction potentials) for the chemicals and functional groups present in the system. The forcefiled development requires quantum mechanical ab-initio simulations. The results of ab-initio simulations, the forcefield parameters, as well and the thermodynamic calculations are presented in Section III. Second, we apply the classical molecular dynamics (MD) simulations to study interactions of characteristic fragments of PEM with water and DMMP and different counterions, potassium, calcium, and aluminum. These simulations are reported in Section IV. Third, we perform large-scale MD simulations to reveal the specifics of nanoscale segregation and molecular mobilities of water and DMMP in sulfonated polystyrene. These findings are

summarized in Section V. Finally, we develop a coarse-grained mesocsopic model of PEM, based on the upscaling of the interaction potentials, and apply the dissipative particle dynamics (DPD). The specifics of membrane morphologies of Kraton, DAIS, and Aldrich sulfonated block copolymers determined by the DPD simulations are described in Section VI. A concise summary of the project results and suggestions for further studies are given in Section VII.

II. Literature review of molecular simulation of PEM.

Most of experimental and simulation studies of sorption and diffusion of water and other solvents in PEM concentrated on Nafion and other perfluorinated ionomers, both in bulk and thin films grafted onto structured substrates. Recent theoretical and simulation works made a significant progress in (1) development of molecular forcefields for Nafion backbone and sidechain [2-4] (2) ab-initio and DFT modeling of Nafion sidechain and its interactions with water [5-9] (3) MM and MD atomistic modeling of solvation of Nafion sidechains and polymer fragments in various solvents, such as water, methanol, water-methanol mixture, and nerve agent simulant dimethylmethylphosphonate (DMMP) [2, 5, 10, 11] (4) MD simulations of nanoscale segregation and diffusion in hydrated Nafion membranes [4, 9, 12-29] (5) modeling of diffusion of water and ions in the vicinity of water – ionomer interfaces [11, 28, 30, 31] (6) development semi-empirical models of proton conduction [15, 16, 27-29, 32] (for reviews, see ref [33, 34]) (7) development of various regular and random network models. [35-37] Other simulation studies of polyelectrolytes on the atomistic level include molecular modeling of poly(ethyleneoxide)sulfonic acid in water,[38] MD modeling of counterion influence on DNA solvation in water [39] and simulations of polyacrylic acid with calcium counterion.[40] Mesoscale approaches to polyelectrolyte modeling included dissipative particle dynamics (DPD) [41, 42] self-consistent field theories,[43, 44] integral equations,[45] cellular automata,[46] and solvent-free MC techniques.[47-49]

In the block copolymers explored as protective membranes, the hydrophilic blocks are formed by sulfonated polystyrene (sPS). Hydrophilicity of sPS depends on the degree of sulfonation. The hydrophobic blocks are made of various polyolefins, such as polyethylene (PE), polypropylene (PP), polyisobutene (PIBL) and polybutadiene (PBD), as well as various quasirandom copolymers (PE-PBD, PE-PP, PE-PIBL, PE-PBD-PS) REFS. Block copolymers composed of immiscible blocks, including block ionomers [50] tend to segregate and form a variety of regular (such as cubic, hexagonal, lamellae etc) and irregular morphologies determined by the block length and the solvent composition. In particular, distinct hexagonal and lamellae morphologies were observed in “parental” (non-sulfonated) polystyrene-polyolefin diblock and triblock copolymers. RDEC researchers [51] found that hydrated sulfonated PS-PB-PS triblocks are segregated also. Kim at al [52] reported a strong segregation in sPS-(PE-PB)-PS copolymer system. However, Gromadzki et al [53] et al observed with AFM that a segregated structure in PE-PS diblock copolymers was lost upon sulfonation, and that spherical micellar formations appeared only upon further hydration in the regions with a high concentration of sulfonic groups.

It remains unclear whether the hydrophilic subphase is homogeneous or segregated itself. We are not aware of any direct investigations into this particular matter. Numerous papers report water sorption and diffusion in sPS of different sulfonation levels, mostly in the acid form. It was established that sPS acid becomes soluble in large quantities of water if the sulfonation level (that is, the ratio of the number of sulfonate groups to the number of benzene rings) exceeds 27% [54]. Water sorption in the polymer increases sharply with the sulfonation level, reaching 350 wt % for fully sulfonated PS (which corresponds to the sulfonation of 100%). Different samples

show significant variations in water sorption and diffusion coefficient, exhibiting dependence of the structure of the procedure of synthesis.

Even less information is available on cation substituted sPS and sPS-polyolefin block copolymers, which are of a greater interest for the protection-related applications. Schneider and Rivin [54] measured sorption and diffusion of water and DMMP in triblock copolymer membranes where the sPS endblocks were separated by hydrophobic blocks composed of polyisobutene, ethylene-butadiene and ethylene-styrene pseudodandom copolymers with H^+, Cs^+ and Ca^{2+} counterions. Sorption and diffusion of both water and DMMP in cation modified samples turned out to be lower than in the acid form of the copolymers. DMMP sorption and diffusion was strongly enhanced by sulfonation (PS only adsorbs 8wt % of DMMP at ambient conditions, while for 100% sulfonated PS DMMP sorption reaches several hundred of wt %) and the activity of water, though this tendency was not as pronounced as in Nafion membranes [54]. Molecular modeling studies of cation substituted sPS are also very limited. Hydration and water diffusion in water soluble sulfonated aromatic dendrimers grafted onto different backbone polymers including polystyrene was recently modeled by Jang and Goddard [4]. This system is somewhat similar to sPS in terms of functional groups present, but differs substantially in skeleton structure and hydrophobicity. The authors considered large (7-8nm) systems and analyzed polymer structuring and water diffusion in the hydrated polymers. The structure analysis showed inhomogeneity at the scale of about 20 to 35 Å. The mobility of water in sPS dendrimers was lower that in Nafion at the same water content.

In this project, we performed a multiscale simulation study of nanoscale segregation and transport/blocking properties of sulfonated triblock copolymers with different counterions solvated by water and DMMP.

Section III. Ab-initio simulation and thermodynamic calculations

III.1. Interactions of the terminal groups of Nafion and sulfonated polystyrene with DMMP

First, we studied the interactions of Nafion sidechain, phenylsupfonate group of sPS, and counterions with water and DMMP. Based on the solubilities of DMMP in Nafion and sulfonated polystyrene-polybutadiene (sSEBS) block copolymers, the RDEC researchers suggested that the solvation of the sulphonate ion differs drastically from that in Nafion membranes (Schneider, private communication). This hypothesis was addressed in the simulations.

For optimization, we used restricted Hartree-Fock (RHF) method with 6-31G* basis. All calculations were done using Baker – Pullay [55] optimization algorithms on a 8-processor Linux cluster from Parallel Quantum Solutions [56]. Two to eight processors were involved in each particular simulation.

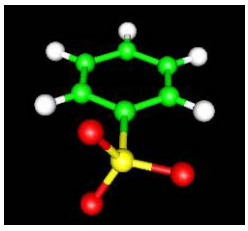

Figure 4. The optimized structure of $PhSO_3^-$ ion

Test optimizations were performed on DMMP molecule, phenol molecule and PhO-anion, CF_3SO_3H molecule, Nafion sidechain, $H_5O_2^+$, and $H_9O_4^+$ complexes. Good agreement with previously reported calculations [6, 57] was achieved. The dipole moment of DMMP was comparable with that calculated from experimental dielectric permeability.

Optimization of $CF_3SO_3^-$ and $Ph\text{-}SO_3^-$ ions Optimization of CF_3SO_3 gives a trivial trans-conformation in agreement with ref [6]. Optimized geometry of $PhSO_3^-$ ion is shown in Figure 4. As expected, one of the SO bonds lies in the benzene ring plane. Natural bond order analysis [58] gives the following local charges –0.29 (C) 2.43911 (S) –1.024 (O), which means that the

group is slightly more polar than in our previous Nafion simulations with a classical forcefield [2, 10, 14].

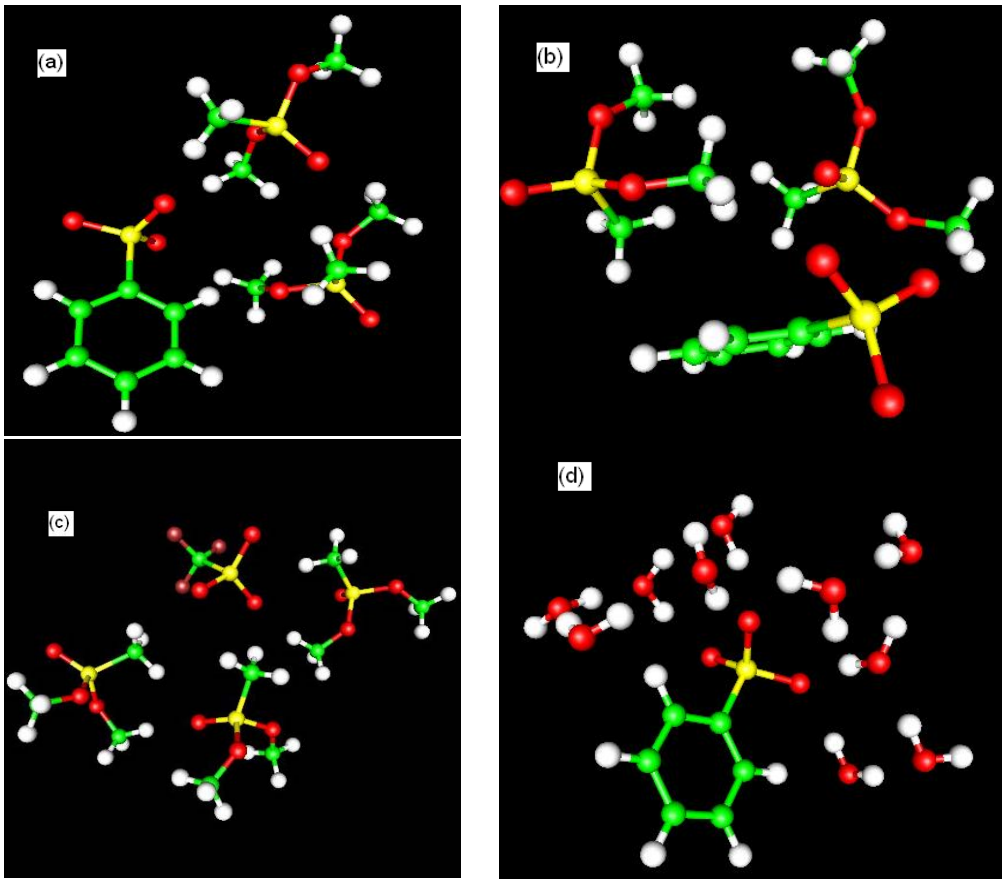

Figure 5 (a) $PhSO_3^-$ + 2DMMP cluster optimized with RHF method (b) $PhSO_3^-$ + 2DMMP cluster optimized with SYBYL classical forcefield [59] (c) $CF_3SO_3^-$ + 3DMMP cluster optimized with RHF method (d) $PhSO_3^-$ + $7H_2O$ cluster optimized with RHF method

As mentioned above, DMMP is a pure solvent for anions like $PhSO_3^-$ since unlike water, it has no protons to donate. Our *ab initio* optimizations revealed no special effect in solvation of the sulfonate in $PhSO_3^-$ compared to $CF_3SO_3^-$. DMMP molecules tend to turn methyl groups to SO_3 oxygens, and the geometry of the cluster reminds of the hydrogen bonds between the methyl hydrogens and SO_3^- oxygens (OH distance of 0.121nm, CHO angle of 160deg). It is worth noting that the the geometry of $PhSO_3^-$ + 2DMMP cluster optimized with the RHF method and with the classical forcefields differ dramatically. RHF optimization shows that DMMP solvates SO_3^- group more readily than the benzene ring (Figure 5).

Interactions of DMMP with proton and potassium cation It was suggested in our previous work [11] that DMMP is a poor solvent for cations compared to water. While the solubility of $PhSO_3K$ in water is expected to exceed significantly the solubility in DMMP, the present *ab-initio* calculations suggest that DMMP interacts strongly with both proton and potassium cation.

Addition of three extra DMMP molecules does not change the nature of proton solvation. The ion (as it was seen in some larger clusters [60]) is located near the cluster surface, and the structure of the $(H{\cdot}2DMMP)^+$ complex is practically the same as in the smaller $H^+{\cdot}2DMMP$ cluster.

Similar complexes are formed between a non-dissosiated R-SO_3H groups and individual DMMP molecules, as shows Figure 6. The proton forms a hydrogen bond to the PO group of the DMMP molecule with HO distance of 0.151nm and OHO angle of 161 deg. The structures are very similar for R = Ph and R = CF_3

a) b)

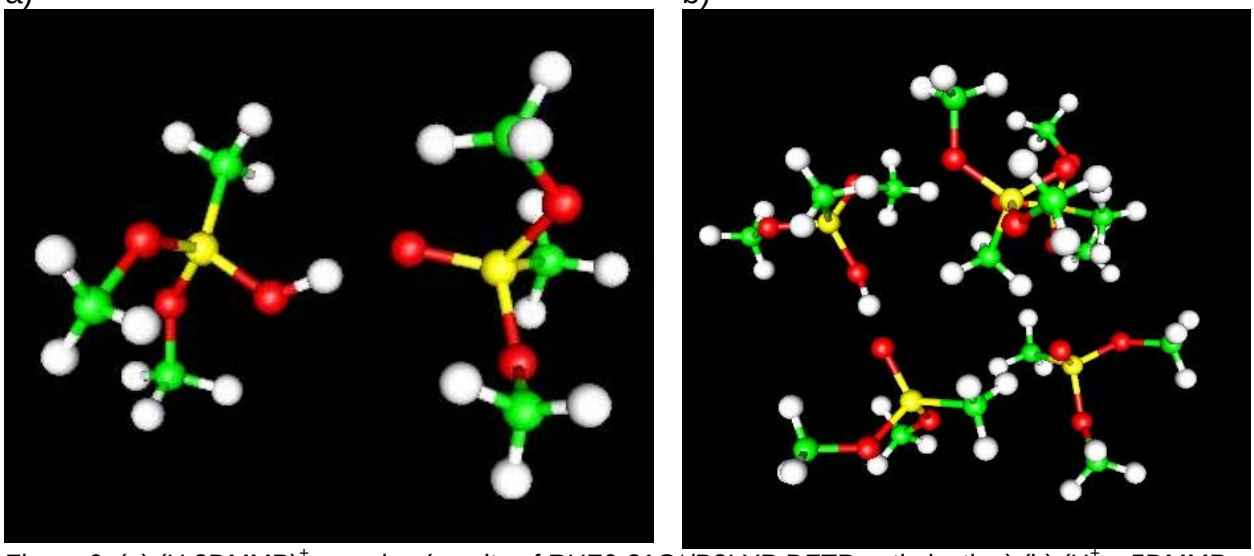

Figure 6. (a) $(H \cdot 2DMMP)^+$ complex (results of RHF6-31G*/B3LYP DFTP optimization) (b) (H^+ + 5DMMP cluster optimized with RHF in 4-31G basis.

Figure 7 shows the optimized structure of $K^+ \cdot 3DMMP$ cluster. Oxygens of the PO groups form a triangle around the potassium ion with K-O distance of 0.22nm. This does not mean a coordination of DMMP molecules by the ion. However, this result suggests a very strong solvation. Addition of two extra DMMP molecules does not change the local structure around the ion, however it is still unclear whether additional DMMP molecules may enter the closest shell.

a) 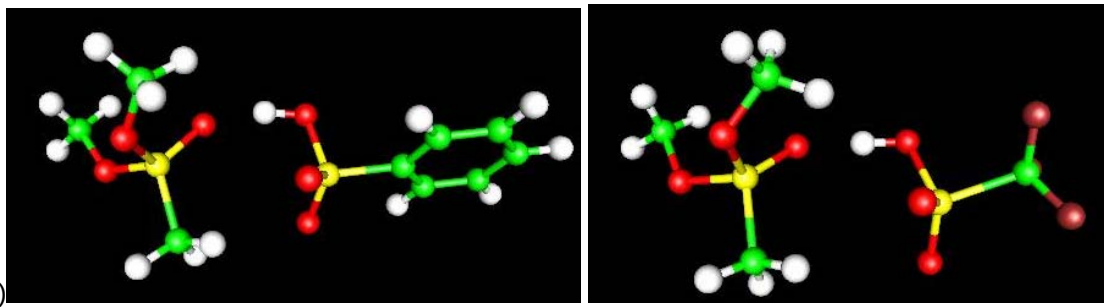 b)

Figure 7. RHF-optimized structures of $RSO_3H \cdot DMMP$ complexes (a) R = Ph, (b) R = CF_3

Geometry optimization and generation of the charge-screening profiles by COSMO.

Because the energy optimization did not reveal a substantial difference in the geometry, we performed thermodynamic modeling based on the ab-initio calculations. Geomerty optimization and generation of the input COSMO files was performed using PQS package on 8-processor PQS Quantum Cube using Restricted Hartree-Fock (RHF) method on TZVP-Ahlrichs basis with BP86 exchange-correlation potential. The calculations took from several minutes on a single processor (for single-atom ions) up to 8 hours on all eight processors (for Nafion

sidechain). When necessary, semiempirical PM3 energy optimization was performed prior to RHF. We compared the final optimized structures with those obtained on a larger 6-31G** basis set with B3YP and OLYP exchange-correlation potentials and existing structures from the literature. Good agreement was obtained for all molecules modeled.

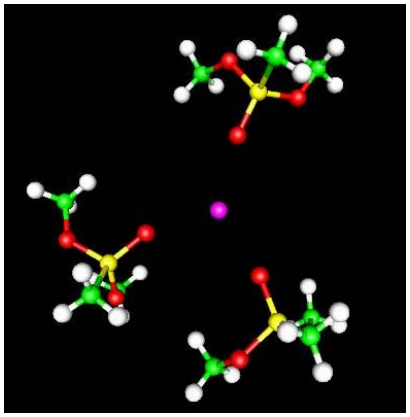

Figure 8. RHF-optimized structures of $(K{\cdot}3DMMP)^+$ complex

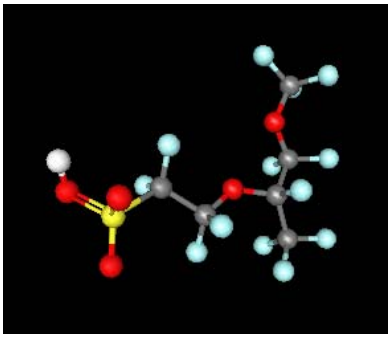

Figure 9 Optimized geometry of Nafion sidechain obtained in TZVP basis, which corresponds well to 6-31G structure reported previously

III.2. Activity coefficients in model electrolyte solutions

From the charge-screening profiles obtained in ab-initio calculations, we calculated the activity coefficients using the Conductor-like screening model (COSMO) as implemented in Cosmotherm package. Figure 10 shows the dependence of DMMP activity coefficient in solutions on the molality of the electrolyte at constant solvent composition (that is, DMMP-to-water ratio). Thus, the mole fraction of DMMP in the solution decreases slightly as the molality of the salt increases. We considered four different compositions of the solvent with DMMP molar fractions x_{DMMP} = 0.01, 0.05, 0.1 and 0.2 (which correspond to DMMP mass fractions of w_{DMMP} = 0.065, 0.266, 0.433, 0.633). It is evident that different ions have a different effect on the activity coefficient of DMMP.

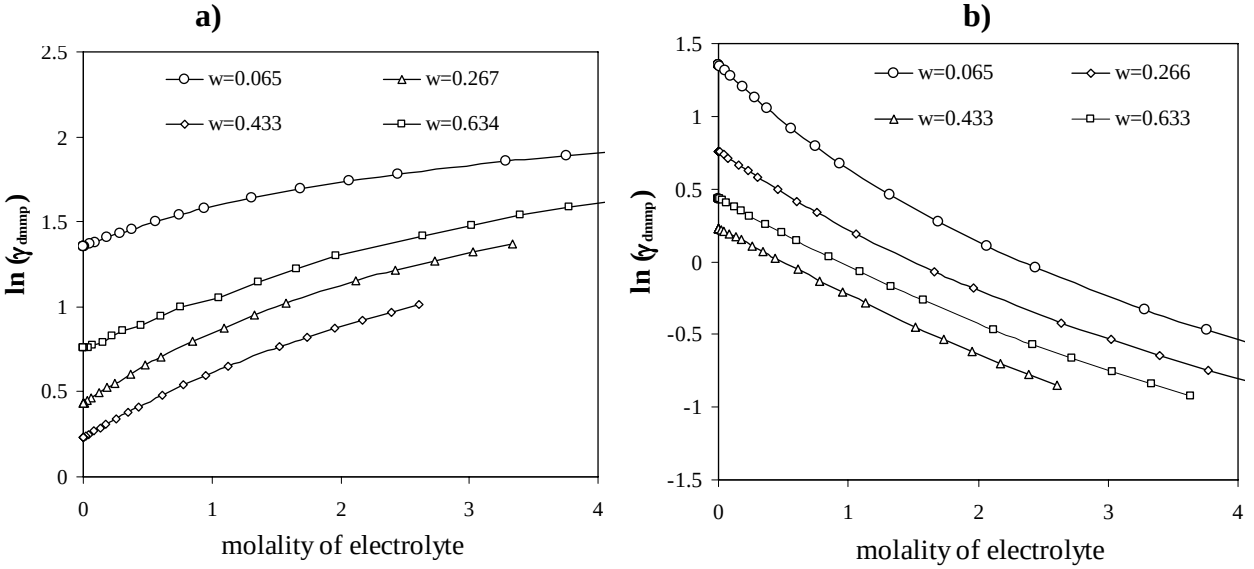

Figure 10. Activity coefficients of DMMP in NH_4O_3S-C_6H_5 (a) and NH_4(nsch) (b) solutions in DMMP/water mixture at different DMMP content

When NH_4O_3S-C_6H_5 is added to DMMP-water mixture, the activity coefficient of DMMP increases steadily (Figure 10a) for all four solvent compositions. If NH_4O_3S-C_6H_5 is replaced by the salt of ammonium and Nafion sidechain (here and further on denoted as NH_4(nsch), DMMP activity coefficient monotonically decreases.

It appears that this qualitative difference should be referred to the different interactions of DMMP with the anion. Figure 11a shows water and DMMP activity coefficients at DMMP mass fraction in the solvent of 0.433. From the Gibbs-Duhem equation one obtains that

$$\sum x_i d\ln\gamma_i = 0$$

For the solution shown in Figure 11a, $\ln[\gamma(m)]$ is approximately linear for both components. From the slope estimates we obtain that $x_{\text{water}} d\ln\gamma_{\text{water}} + x_{\text{DMMP}} d\ln\gamma_{\text{DMMP}} = 0$. In the contrary, in NH_4(nsch) solutions there is no strong correlation between water and DMMP activities (Figure 11b).

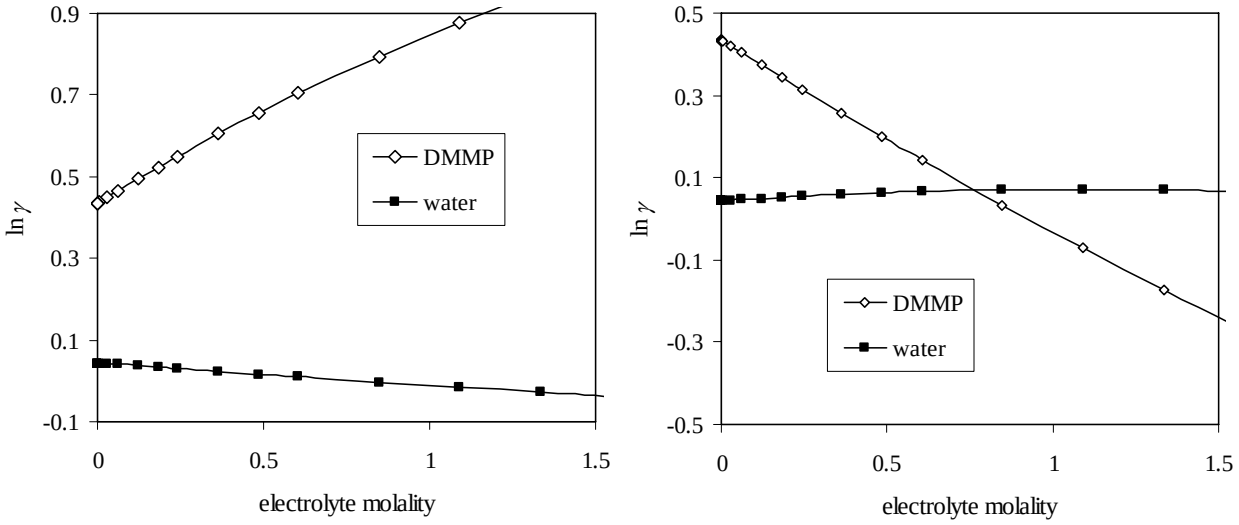

Figure 11. Water and DMMP coefficients in NH_4O_3S-C_6H_5 (a) and NH_4(nsch) (b) solutions at DMMP mass fraction of 0.433

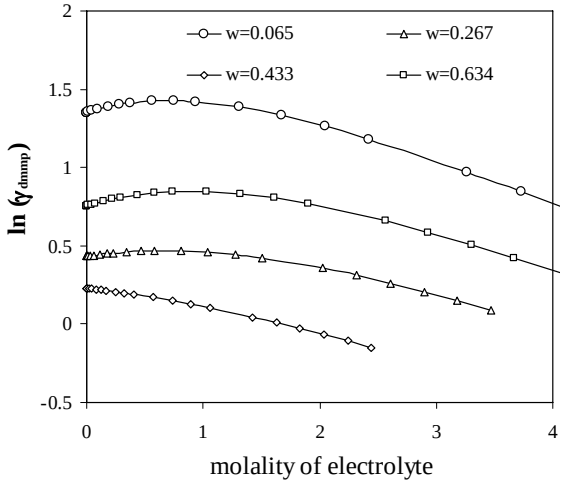

Figure 12. Activity coefficients of DMMP in $NH_4O_3SCF_3$ solutions in DMMP/water mixture at different DMMP content

parts of the anion. This observation should be explored further. In order to explore the hypothesis of the reduction electronegativity of the sulfonate anion by CF bonds (put forward by Dr. Schneider, RDECOM, Natick, personal communication) we also modeled the interaction of DMMP and water with NH_4O_3S-CF_3. It turned out that the DMMP activity coefficients exhibit maximum at m = 0.8 for small DMMP content and monotonously decreases at highest DMMP content (Figure 12).

Since water interacts strongly with SO_3 group rather than with the benzene ring (benzene-sulfonic and *p*-toluene-sulfonic acids are strong acids well soluble in water while benzene is almost insoluble) our observation may indicate that in NH_4O_3S-C_6H_5 solution water and DMMP tend to compete for the interaction with ionic groups, while in NH_4(nsch) they attack different

The influence of the cation

Since DMMP interacts strongly with different cations, the activity of DMMP depends on the type of cation. Ammonium cation is able to form up to four hydrogen bonds with DMMP molecules as shown in Figure 10. Interestingly, the interaction with the ammonium atom seems to affect the DMMP minimum conformation: the conformation of both DMMP molecules in Figure 13 does not correspond to either of the main minima of DMMP in vacuum and is unstable in the RHF minimization of a single DMMP. Replacement of ammonium cation by sodium leads to an increase in the DMMP activity coefficient (Figure 14), but no qualitative changes were observed: the DMMP activity coefficient increases monotonically with the molality.

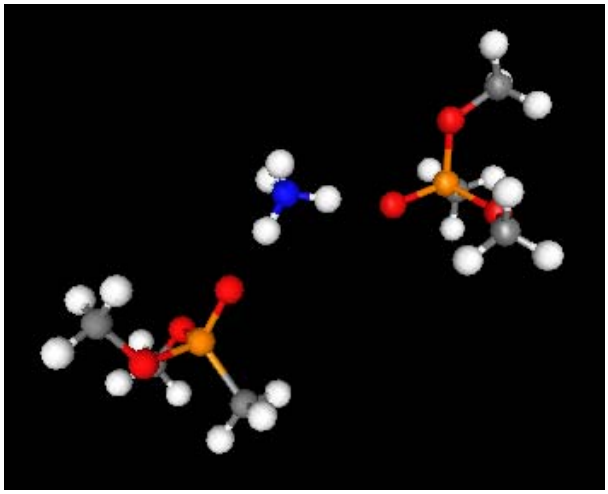

Figure 13. Optimized structute of $(NH_4*2DMMP)+$ ion. Note a change in DMMP conformation compared to an isolated DMMP

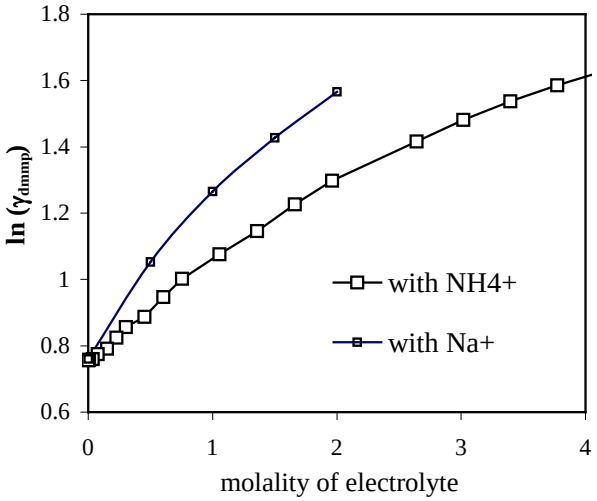

Figure 14. DMMP activity coefficients in NH_4O_3S-C_6H_5 and NaO_3S-C_6H_5 solutions at w_{DMMP}=0.267

III.3. Construction of the forcefield for phenylsulfonate group.

MD simulations of arenes and polyethylene has been reported in the literature; both all-atom and united-atom molecular forcefields have been developed for this class of molecules. [61-63] However, no suitable forcefields were developed for sulfonated arenes, and we had to calculate new parameters specific to this class of systems. In order to assign the point charges to the atoms, we performed a restricted Hartree-Fock (RHF) minimization of benzenesulfonate anion $C_6H_5SO_3^-$ and 2,4-diphenylpentane. In order to evaluate the point charges and the rigidity of the covalent CCS, CSO and OSO angles, we performed RHF minimization of benzenesulfonate ion with PQS ab-initio. [56] Then, the parameters of the bending potentials were fitted to the directions and oscillation frequencies of sulfur and oxygen atoms. The parameters are discussed in section IV. The CCSO torsion that determines the rotation of the sulfonate group around the CS bond is of a special interest. Benzenesulfonate ion has two major conformers: one has a *cis*- CCSO angle (one of the oxygens is located in the benzene ring plane) and the other has a straight CCSO torsion angle (one of the CGSO planes is perpendicular to the benzene ring, the other two form 31.5deg angles with the ring plane). The latter is 0.16 kJ/mol

less stable than the former. We fitted the parameters of the standard OPLS potential for torsion angles $U_{tors}(\theta)=½(1+K_1\cos\theta)+½(1-K_2\cos 2\theta)+½(1+K_3\cos 3\theta)+½(1-K_4\cos 4\theta)$ to the energy difference between the conformations. The parameters obtained are presented in Table 2.

III.4. Ab-initio studies of the conformation of the arene backbone.

To explore "natural" conformations of the backbone, we identified characteristic conformers of 2,4-diphenylpentane (Figure 15), chosen as a representative fragment of the sPS block. 2,4-diphenylpentane is a symmetric substituted alkane that has two asymmetric carbons: C2 and C4 atoms have four different substitutes each. As a result, the alkane has two different isomers with different conformations. For example, conformations depicted in Figures 2A1 and 2B1 are different, asymmetric, and they cannot be obtained from each other by any sequence of internal rotations or mirror imaging; this can only be done by changing the substitute order at C_2 and/or C_4 carbons (in this way they are similar to enantiomers). Figure 16 depicts four major conformations for each isomer. We discern the conformations by two factors (1) the elongation of the backbone that is determined by C_1-C_2-C_3-C_4 and C_2-C_3-C_4-C_5 torsion angles (for atoms denotation see Figure 15) and (2) the distance between the benzene rings determined by C_{2B}-C_2-C_3-C_4 and C_{4B}-C_4-C_3-C_2 torsions for each pair of the main torsion angles of the aliphatic backbone. The main torsion angles and energies are given in Table 1. The difference between the conformer reaches 26 kJ/mol for isomer A and 21 kJ/mol for isomer B. The locations of the benzene rings with respect to each other are qualitatively different for the two isomers. In both more stable conformations of isomer A (Figures 16A1 and 16A3), the benzene rings are almost parallel; these conformations are possibly stabilized by the π–π interactions between the rings. They correspond to *trans-trans* (most elongated) and *gauche-gauche* (least elongated) conformations of the aliphatic backbone. On the other hand for isomer B, the "folded" conformations with the phenyl group parallel to each other are less stable; the "extended" (more stable) conformations have *trans-trans* and *trans-gauche* pairs of the main angles.

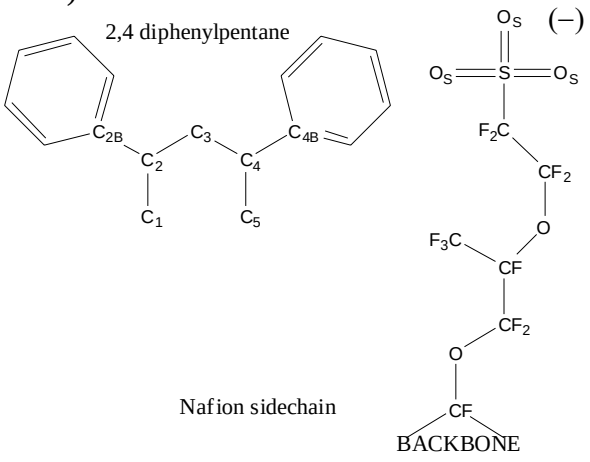

Figure 15. Chemical formulae of 2,4 diphenylpentane and nafion sidechain

Thus, we may conclude that the configuration and flexibility of the polymer depends substantially on the order of substitutes at the carbons, to which the phenylsulfonate groups are bonded. In this work, the sPS fragments have a random order of substitutes at each atom; therefore, both all conformation types should be present. The sPS backbone is supposed to favor *trans* backbone angles although Table 1 shows that the angles are distorted considerably from the "normal" positions of 180 deg for trans and 60 deg for gauche configurations.

Table 1. Torsion angles and energies of main conformers of 2,4-diphenylpentane shown in Figure 16. Two isomers differ by the order of substitutes at 2,4 asymmetric carbons

Conformer		Torsion angles, deg				E-E_0, kJ/mol
		C1-C2-C3-C4	C5-C4-C3-C2	C2B-C2-C3-C4	C4B-C4-C3-C2	
A1	B3LYP	158.8	158.8	-76.1	-76.1	0
ttgg	TRAPPE	167.4	167.4	-67.8	-67.8	0
A2	B3LYP	-161.6	71.6	-74.0	-58.9	+1.0
tggg	TRAPPE	-172.8	67.2	-70.8	-61.1	+2.3
A3	B3LYP	95.7	68.9	139.6	-60.8	+4.2
ggtg	TRAPPE	104.2	65.4	151.0	-59.2	+2.9
A4	B3LYP	80.3	49.8	52.5	82.7	+26.6
gggg	TRAPPE	66.1	54.3	56.8	80.0	+33.0
B1	B3LYP	172.7	172.7	-62.1	-62.1	0
ttgg	TRAPPE	173.3	173.3	58.7	58.7	0
B2	B3LYP	-48.9	169.5	82.5	-65.9	+21.2
gtgg	TRAPPE	-54.2	173.3	77.4	-64.6	+17.4
B3	B3LYP	-62.8	97.1	66.9	-138.2	+19.4
gggg	TRAPPE	63.7	101.8	60.4	-144.5	+21.1
B4	B3LYP	176.6	64.6	59.1	170.0	+2.7
tggt	TRAPPE	176.5	63.3	57.8	174.4	+4.6

III. 5. Discussion. Ab-initio and thermodynamic modeling of water and DMMP interaction with phenylsulfonate group was performed in comparison with Nafion sidechain. We conclude that DMMP strongly interacts with both sPS and Nafion in the acid forms accepting a hydrogen bond from the terminal -SO_3H group. Furthermore, DMMP has a potential to become protonated and form complex cations that include a proton, water and DMMP molecules. DMMP interacts strongly with alkali metal cations and competes with water for the first solvation shell of the metals. These tendencies are probably common for phosphororganic CWA. We also confirmed the suggestions of RDEC chemists that water and DMMP are likely to attack different groups of the sidechains in hydrated Nafion, but appear to compete more strongly for the first solvation shells of the sulfonate groups in hydrated sPS. This is a positive sign indicating a better potential for sPS base block-copolymer membranes over Nafion as protection membranes.

The other aim of our ab-initial studies was the construction and testing of the classical forcefields for MD simulations. They are discussed in the next section.

IV. Molecular dynamics study of the solvation of sulfonated polystyrene and Nafion fragments in water, DMMP and their binary mixturte.

We explored the solvation and dynamics of sulfonated polystyrene in water and DMMP to elucidate the mechanicsms of DMMP sorption in the membranes.

IV. 1. Systems and Methods.

Sulfonated polystyrene fragments, counterions, and solvents**.** Tactic sPS fragments were composed of 10 and 20 monomer units. Each fragment was terminated with a methyl group at one end and a $PhSO_3^-$ group at the other end. The sulfonation was 100%, i.e. the sulfonate group was attached to every phenyl in *para*- position. We assumed a random order of substitutes at aliphatic carbons, to which the phenyl groups were bound, since this order is not controlled in PS

synthesis. To explore the interactions of sPS in hydrophilic subphase of swollen triblock copolymer membranes, we considered solvation of sPS fragments in water, DMMP and water-DMMP 1:1 and 2:1 (by volume) binary solvents. Counterions studied experimentally in ref [54] were considered: potassium K^+, calcium Ca^{2+} and aluminum Al^{3+} (see Table 1). To preserve the electro-neutrality in the systems with Al^{3+} counterion, three Al^{3+} ions and one K^+ were added to 10-monomer fragments. This ratio roughly mimics the actual situation in cation-substituted sPS, since the exchange capacity of both sPS and Nafion membranes to aluminum cation never reaches 100% .[54]

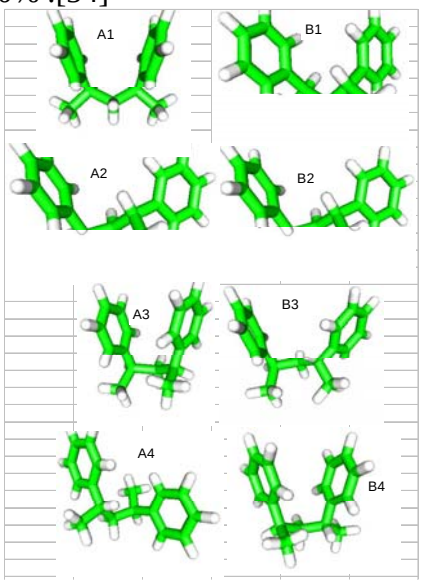

Figure 16. Conformers of 2,3-diphenylpentane optimized in RHF with 6-31g++ basis, B3LYP exhange correlation functional . Left: isomer A; right: isomer B.

For comparison, we also modeled 4-unit tetrafluoroethylene-perfluoro-3,6-dioxa-4-methyl-7-octenesulfonate oligomers (typical fragments of Nafion polymer, similar to those modeled in ref [2]) with K^+ counterion in pure DMMP, since this system was not reported previously. Neighboring sidechains were separated by eighteen CF_2 groups that corresponds to the equivalent polymer weight of 1165. In each simulation, we introduced the number of solvent molecules to achieve the approximate cell volume of $2.7 \cdot 10^4 Å^3$ (box size of 30Å) with 10-monomer sPS and Nafion, and $6.4 \cdot 10^4$ $Å^3$ (box size of 40Å) with 20-monomer sPS.

Simulation techniques. The models of sPS and Nafion fragments were constructed and optimized using the Materials Studio package from Accelrys. [64] The conjugate gradient method with the maximum atomic displacement of 0.1 Å was used for minimization. MD simulations were carried out at T = 303 K and 1atm. Lennard-Jones and electrostatic potentials were cut off at 14Å. To account of long-range electrostatic interactions, the Ewald summation was applied. The temperature and pressure were maintained by the Nose-Hoover thermostat. [65, 66] The equations of motion were solved by the double-timestep Tuckerman [67] scheme, with the fast-fluctuating forces integrated with 0.2 fs timestep and slower fluctuating forces integrated with 2 fs timestep. All MD simulations were performed using MdynaMix5.0 software package. [68, 69] Gopenmol program [70] was used for visualization of the results.

In the initial configuration of MD simulation, fragment molecule was placed in a cavity, surrounded by solvent molecules, which were arranged as a face centered cubic lattice at a low density of 0.05 g/cm^3. During the first 70 ps of the simulation trajectory, the cubic simulation box was gradually compressed until the desired density of 0.8 g/cm^3 was reached. The compression was followed by a 40 ps NVT simulation with the oligomer molecule kept rigid, to establish a preliminary equilibrium in the solvent. Then the simulation was carried out in the NPT ensemble at the atmospheric pressure. The total length of the simulations was 5ns for Nafion and 10 monomer sPS fragments and 7ns for 20-monomer sPS fragments (Table 2). Every

100 fs the configuration of the whole system was saved for further analysis, which was performed with the TRANAL program of MDynaMix 5.0 package [68, 69].

Table 2. The list of systems modeled.

Fragment*	mono-mers	Counter Ions	Solvent			Averaging time, ns
			Composition	N_{H2O} †	N_{DMMP} †	
SPS	10	10 K^+	Water	750		4 ns
SPS	20	20 K^+	Water	2000		6 ns
sPS	20	20 K^+	DMMP		420	6 ns
sPS	10	10 K^+	Water+DMMP (1:1 vol)	375	53	4 ns
sPS	10	5 Ca^{2+}	Water	750		4 ns
sPS	10	5 Ca^{2+}	Water+DMMP (1:1 vol)	375	53	4 ns
sPS	10	$3Al^{3+}$+K^+	Water	750		4 ns
sPS	10	$3Al^{3+}$+K^+	Water+DMMP (2:1 vol)	475	35	4 ns
Nafion	4	4 K^+	DMMP		420	4 ns

* the sequence of substitutes at asymmetric atom was RRSSRSSRRSR in 10-mers and RRSSRSSRRSRRRSSRSSRRSR in 20-mers from the "head" (terminal methyl group); the seniority sequence of the substitutes is head, tail, phenyl, hydrogen

† number molecules of that component

IV.2. Molecular forcefields.

Sulfonated polystyrene**.** MD simulations of arenes and polyethylene has been reported in the literature; both all-atom and united-atom molecular forcefields have been developed for this class of molecules. [61-63] However, no suitable forcefields were developed for sulfonated arenes, and we had to calculate a few new parameters specific to this class of systems. The total potential energy of the system was represented as a sum of Lennard-Jones (LJ), Coulombic, covalent bond stretching, angle bending, and dihedral energy terms. United atom LJ from forcefield [63] was employed to describe the van der Waals interactions. The LJ parameters for the sulfonate group were taken equal to those in Nafion. [3] Fitting the parameters missing in literature is decribed in section III.3. All covalent bonds were kept rigid using SHAKE algorithm, [71] and the contribution to the potential energy coming from the bond stretching was omitted in this work. The equilibrium bond distances for the hydrocarbon backbone and phenyl groups were taken according to TRAPPE forcefield; [63] the length of the C-S and S=O bonds were taken equal to those in minimized Ph-SO_3^- structure. Covalent angle stretching was described by the simple harmonic potential $U_{\text{angle}}(\theta) = \frac{1}{2}K_\theta(\theta-\theta_0)^2$. For aliphatic backbone and benzene rings, we used the parameters from ref [63]. In order to evaluate the rigidity of the covalent CCS, CSO and OSO angles, we performed an RHF minimization of benzenesulfonate ion with PQS ab-initio. [56] Then, the parameters of the bending potentials were fitted to the directions and oscillation frequencies of sulfur and oxygen atoms. The parameters are given in Table 3. The torsion angles of the hydrocarbon backbone were also taken from ref [63]. The phenyl rings were kept rigid using out-of plane "improper" torsion potential functions in the standard harmonic form $U_{\text{impr}}(\phi) = \frac{1}{2}K_{\text{impr}}(\phi-\phi_0)^2$. In gerenal, we found that the TRAPPE forcefield describes reasonably the conformations of the backbone polymer: major conformations and corresponding energies are reproduced with a sufficient accuracy (Table 1).

Table 3. Parameters of the forcefield

Point charges, electrons					
CH3	0	CH2	0	CH	0
CB1	-0.03	CB2(5)	-0.02	CB3(4)	-0.23
CB4	-0.230	S	1.755	O	-0.75

Counterions	**σ, Å**	**ε, kJ/mol**	**ref**
K^+	3.36	0.568	[72]
Ca^{2+}	3.44	0.5	[73]
Al^{3+}	3.95	0.505	[74]

Bonds:	K, kJ/mol/ Å)	r_0 , Å
C_B-S	1400	1.85
S-O	2260	1.66

Covalent angles			CCSO dihedral parameters, kJ/mol/rad^2
Angle	θ_0 deq	K,kJ/mol/rad^2	
CSO	103.8	235	K_1= 3.1 K_2= -9.4
OSO	114.8	421	K_3= 5.8 K_4= 0

Improper torsion *	K_{impr}, kJ/mol/rad^2	ϕ_0, deg
C_B-C_B-C_B-C_B	400	0
C_B-C_B-C_B-X	400	180
X- C_B-C_B-X	400	0

* C_B: an aryl carbon; X: a substitute

Counterions and solvents. Counterions were modeled as charged LJ centers. The LJ parameters for K^+ and Ca^{2+} counterions were taken from refs [72] and [75] respectively. For Al^{3+} cation we simply used the LJ parameters from generic Universal Forcefield. [74] Central potentials of LJ type cannot adequately describe interactions of aluminum ion with water and DMMP, which forms coordination compounds with water, such as $[Al(H_2O)_6]^{3+}$ complex (the energy minimum for the interaction of Al^{3+} ion with water corresponds to the distance of 1.76Å between the metal and oxygen atoms according to ref [76] and our own DFT calculations). However, the LJ model is capable of reproducing important features of the systems under consideration related to a general behavior of a tri-valent cation capable of associating with the sulfonate groups. Water was modeled using SPC/E rigid model.[77] The molecular forcefield for DMMP was developed in our earlier work. [3]

IV.3. Polymer – solvents interactions.

Backbone conformations and stiffness**.** Solvated molecules do not have to repeat the conformations they exhibit in vacuum, especially in the presence of strong electrostatic interactions of sulfonate groups with water and counterions. In our simulations, aliphatic torsion angles exhibited distorted *trans* conformations predicted by the RHF optimization (Section IV.1). For example, Figure 17 shows the distribution of torsion angles of the aliphatic backbone of 10-monomer sPS fragments in water with potassium counterion. The number in the legend shows the particular angle on the backbone; dihedral angles are numbered starting from the terminal CH_3 group (Figure 15). The angle distribution shows preference to A1, A2 and B4 conformations of the backbone aliphatic chain (see also Table 1, Figure 16), for which the distorted trance (± 150-170deg) and regular (± 60deg) gauche angles are typical. However, a

number of less stable conformations with "normal" *trans* torsions (typical for B1 conformer) was also present. The backbone was rather stiff: most torsion angles experienced not more than one transition within the entire 4ns simulation period. In average 0.2 transitions per 1ns was detected in 10-monomer sPS fragments with water as a solvent and K^+ as counterion.

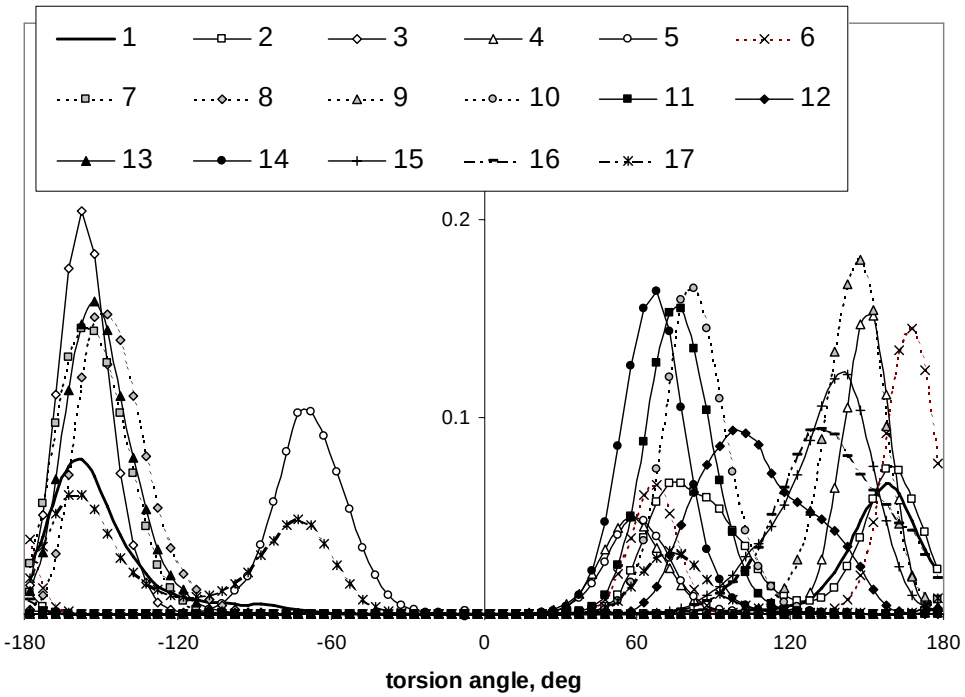

Figure 17. The distributions of the aliphatic backbone dihedrall angles in sPS 10-mer in water with K+ counterion. The number on the legend show the number of the torsion in the aliphatic chain starting from the terminal CH3 group: the backbone of the olygomer consists of 20 carbon atoms and 17 C-C-C-C dihedral angles.

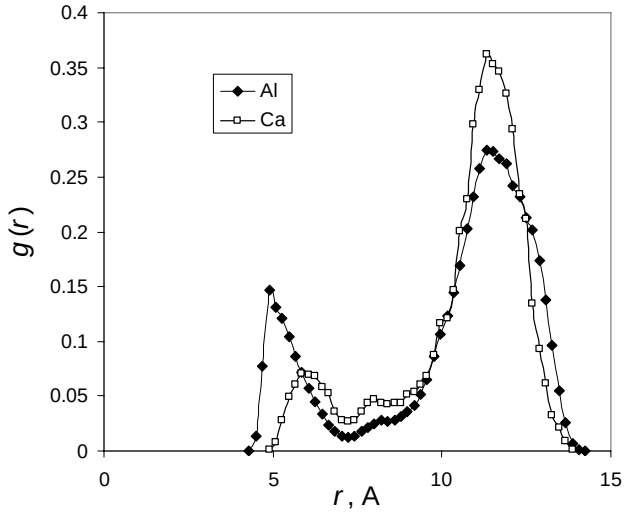

Figure 18. Intremolecular RDF between the sulfur atoms bonded to the neighboring phenyl groups of 10-monomer sPS oligomer with Ca^{2+} and Al^{3+} counterions.

Effect of the counterion**.** It is expected that the counterion may substantially influence the conformations and flexibility of the sPS backbone. We did not observe any visible change of flexibility and conformations when K^+ counterion was replaced by Ca^{2+}. However, the sPS backbone behavior with Al^{3+} was quite distinct. Figure 18 shows the intramolecular radial distribution function (RDF) for sulfur atoms attached to neighboring phenyl rings (intramolecular RDF is the probability distribution of finding the two atoms at certain distance from each other). The first peak at 4-7Å corresponds to "folded" conformations, that is, it is typical for conformations A1, A4, B3, B4 in Figure 16. The second peak is broad. It corresponds to "extended" conformations (A2, A3, B1, B2 is Figure 16). For example, the distance between the neighboring sulfur atoms is 12Å in conformation B2. Extended conformations prevail; however, when Ca^{2+} counterion is replaced by Al^{3+}, the fraction of the folded conformations approximately doubles and the first peak shifts from 6Å to 4Å. We attribute the change in conformations to different behavior of counterions. Both K^+ and Ca^{2+} are mostly dissociated from the sulfate groups, the Al^{3+} ion is associated, which is demonstrated by sulfur-counterion RDFs for K^+ and Al^{3+} shown in Figure 19 (the *intermolecular* RDF is the local concentration of atom *i* at certain distance *r* from atom *j* related to the average concentration of the former). The RDFs for K^+ and Ca^{2+} counterions are typical for liquid solutions; the RDF for Al^{3+} counterion shows to very high peaks corresponding to the counterion location either in the "palm" of the sulfonate group or on the periphery between two oxygens. The integration of the RDF shows a 98% probability of finding Al^{3+} counterion in 5Å vicinity of the sulfur atom. This has double effect on the conformation: (i) because three sulfonate groups are needed to neutralize a single Al^{3+} counterion, strong electrostatic forces cause a distortion of the backbone (ii) counterion dissociation critically alters the sidechain solvation by solvent molecules, since they inetreact with an anion rather than with effective cation or dipole. Al^{3+} ions surrounded by three sulfonate groups were observed rarely, because the electrostatic forces are not sufficient to overcome the energy barriers needed to fold a single backbone fragment to such an extent.

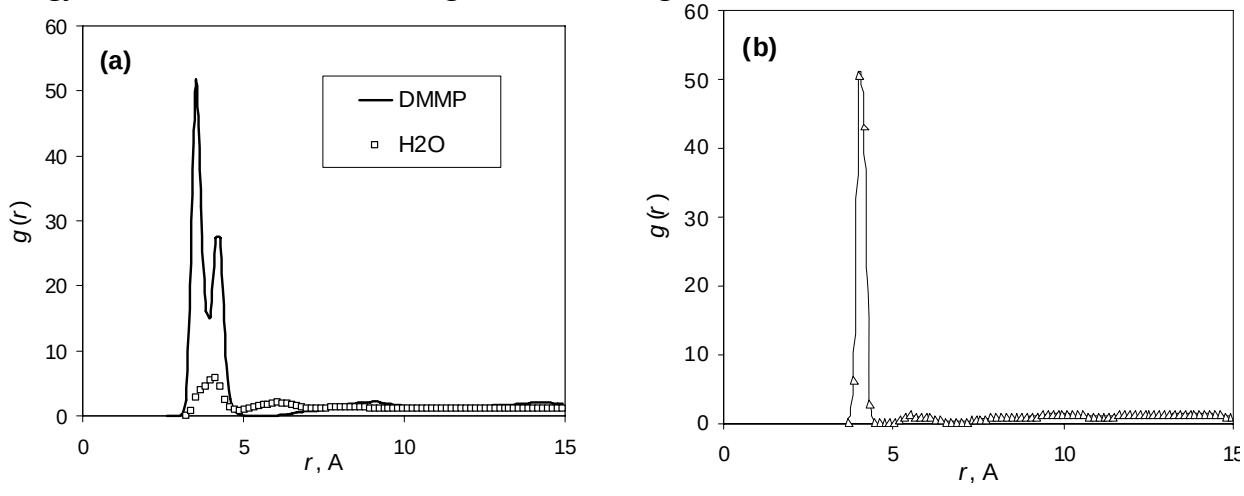

Figure 19. RDF between the sulfur of sulfonate groups and counterions in solutions of 10-nomomer sPS olygomers. (a) K^+ counterion in water and DMMP (b) Al^{3+} counterion in water

In the hydrophilic phase of the bulk material, the neutralization is more readily achieved, because any ion may be surrounded by sulfonate groups belonging to different chains. Nevertheless, the gain in torsion energy may be quite significant. This effect explains why sPS with three-valent

counterions exhibits a notable osmotic uptake of salt solutions: [54] the extra salt resolves the need for counterion neutralization.

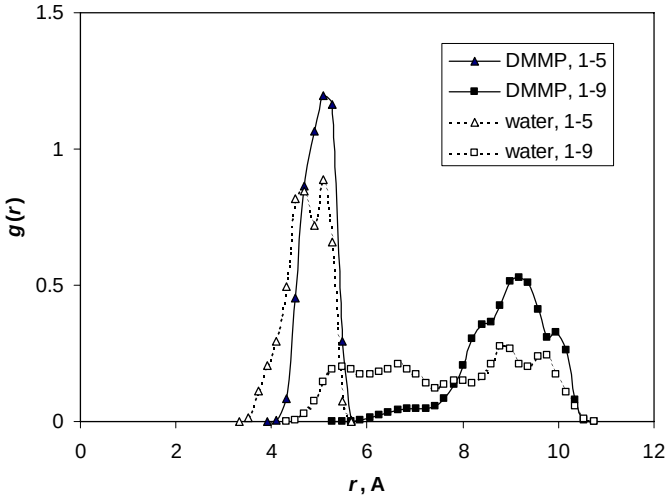

Figure 20. Intra-molecular radial distribution functions for sPS 20-monomer olygomer in DMMP (closed symbols) and water (open symbols). The RDF is the average of all pairs of aliphatic chains with even numbers (I.e. the backbone carbons phenyl rings are attached to) separated by four (1-5 neighbours) and eight (1-9 neigbours). It is clear that the olygomer is stiffer in DMMP than in water.

Effect of the solvent**.** In pure DMMP, the counterions are always associated with sulfate groups, as DMMP is an inferior solvent for the counterions compared to water (for RDFs for K^+ with sulfur is shown in Figure 19). In general, DMMP makes the backbone much stiffer. For example, the backbone of 10-monomer fragment with K^+ counterion showed 0.1 transition per aliphatic bond per 1ns in pure DMMP, which is twice as less often as in water. Figure 20 displays the intramolecular distribution functions between the backbone aliphatic carbons separated by four and eight covalent bonds. The RDFs show that the predominance for the *trans*-configurations of the backbone is much stronger in DMMP, where the RDF for the atoms separated by eight bonds show a distinct peak corresponding to 9.1Å, which is nearly twice the distance for the peak of the RDF for carbons separated by four covalent bonds. A very different situation is observed in water, where RDFs show a variety of conformations.

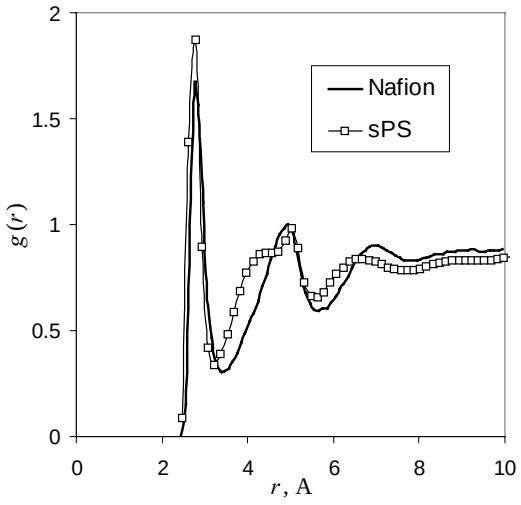

Figure 21. Radial distribution function for oxygens of sulfonate groups and water in queous solutions of 10-monomer sPS olygomer and 4-unit Nafion olygomer with K^+ counterion.

This observation agrees with the practical use of DMMP as deplasticizer for polymers. [78-80] This deplasticizing effect is most visible for Nafion. Both backbone and sidechain flexibility were less pronounced than in water, methanol, or binary mixture modeled in refs [2, 14]. Even in water-DMMP 1:1 vol binary solvent the deplasticizing effect of DMMP is quite pronounced: the backbones of sPS fragments were generally stiffer than in pure water. It is natural, since the backbone is surrounded by DMMP and only sulfonate groups and counterions are mostly solvated by water.

IV.4 Solvation of the sulfonate groups.

Solvation in water**.** As was described in details in refs [2, 14], water intensively interacts with sulfate groups via hydrogen bond donation. In this section, we analyze the difference between water interaction with the sulfonate groups of Nafion and sPS. Figure 21 shows the RDFs for oxygen atoms of water and those of sulfonate groups of the two polymers. The two RDFs are very similar. The first peak of the RDF is observed at about 3Å, which corresponds to the oxygens of water molecules that form hydrogen bonds to the sulfonate group [2, 10] is somewhat higher in sPS solution. The geometrical analisys for hydrogen bonding similarly (a bond is formed if the distance between the donor and acceptor oxygens is below 3.4A and the OHO angle exceeds 120deg [39, 81]) showed 5.4 hydrogen bonds for sulfonate group (with K^+ conterion), compared to 5.1 obtained in ref [2] (it should be noted that Na^+ cation was considered in ref [2]). The hydrogen bond lifetimes can be compared on the basis of the characteristic times of water molecules residence near the oxygens of sulfonate groups. We assumed the residence of a water molecule at a certain sulfonate group is established, when the distance between two oxygen atoms belonging to solvent molecules and an oxygen of a SO_3^- group remained shorter that 3.4 Å within 2 ps. The residence was considered terminated, when this distance exceeded 3.55 Å or when it remained larger than 3.4 Å within 2 ps. [39, 81] The residence time estimate was based on the assumption that the probability of a hydrogen bond to be destroyed within time t can be presented as $1-a\exp(-bt)$. Unlike the hydrogen bond numbers, the residence times do not involve the OHO angle as a criterium; however, since most of stable contacts between negatively charged oxygen atoms originate from hydrogen bonds, the residence times give valuable information on the hydrogen bonding dynamics. The hydrogen bonds between water and sPS sulfonate groups appeared more stable than between water and Nafion sidechain (11.4 vs 8.3 [2]), however the difference is not significant. In both cases, hydrogen bond lasted over several rotation times of water molecule in the pure liquid (about 2.8ps [3, 82]).

The RDF for sPS shows a small but pronounced and reproducible peak at ca 5Å, which indicates a strong anisotropic structuring. This structuring is demonstrated by spatial distribution functions (SDF). SDF is a three-dimensional density profile, calculated in a reference coordinate system, rigidly attached to a part of the molecule of interest. For a better visualization, we built the reference coordinate systems on two OS vectors of each sulfonate group. The SFDs obtained for all side chains of each fragment were averaged.

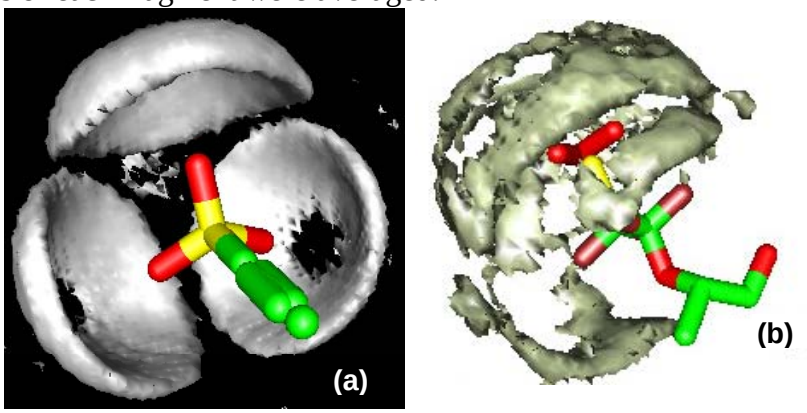

Figure 22. Spatial distribution functions of water oxygens around the phenylsulfonate groups of sPS (a) and Nafion (b) in aqueous solutions with K+ counterion. The sticks show the position of the atoms of phenyl group averaged in a coordinate systrem rigidly attached to two of S-O vectors; gray clouds show the locations where the average local density of water oxygens in 2.5 or more times greater than the average.

Figure 22 shows the coordinates of the atoms of the $PhSO_3^-$ group in the reference system averaged over the simulation trajectory and the regions were the average local density of the water oxygens is 2.5 times as large as the average number density of the solvent. For comparison, we give a similar picture for Nafion (from ref [2]). Because of the sulfonate group rotation around the C-S bond and the rigidity of the phenylsulfonate construction, the average locations on all carbons of the phenyl group as well as the aliphatic carbon, to which it is bonded, all fall onto the same straight line (Figure 23). In both Nafion and sPS solutions, the first solvation shell is clearly observed and the second solvation shell is hardly visible. It is clear that the solvation shell around $PhSO_3^-$ group of sPS shows a strong anisotropic order, forming three distinct clouds corresponding to three oxygens of sulfonate group. This behavior is somewhat similar to that observed in Nafion solution in methanol [10] but the structuring in sPS-water systems is more pronounced.

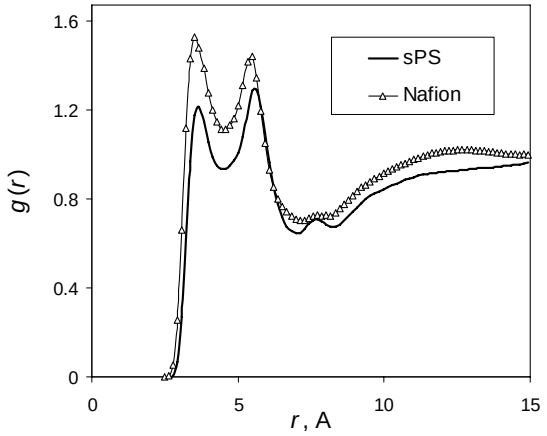

Figure 23. Radial distribution functions between the oxygen atoms of SO_3^- group of sPS and Nafion olygomers and the O_P oxygen of DMMP which is binded by a double bond to the phosphorus atom. The counterion is K^+.

Solvation in DMMP**.** A similar comparison between Nafion and sPS solvated in DMMP was performed. The RDF between sulfonate and O_P oxygens (the oxygen of DMMP connected to the phosphorus by a double bond, Figure 15) with K^+ counterion are shown in Figure 23. (It appears that RDF in Nafion is larger than in sPS within the entire range of distances shown; the only reason for that is the volume fraction of the polymer being different in the two simulations; this fact should therefore be ignored). Again, the RDFs for Nafion and sPS are very similar. The counterion is associated; it is located in the vicinity of the group (Figure 19), forming a very strong dipole. The dipoles of DMMP molecules are oriented respectively around the $SO_3^-K^+$ dipole. The first peak of the RDF is observed at the distance of 3.4Å, which is close to that in water. The only situation we can suggest is that O_S, O_P and K^+ atoms are all adjustent to each other. It is likely that the second peak corresponds to two other oxygens of the sulfonate group. For sPS in DMMP, the second peak is higher than the first peak showing that the solvation shell of phenylsulfonate group of sPS has a greater anisotropy than in Nafion.

This suggestion is confirmed by the SDFs of differenrt atoms of DMMP and the counterion around the sulfonate group. The SDFs for the potassium counterion in sPS solution in DMMP show two disctinct places where it could be located: either near an individual oxygen atom of the sulfonate group or at an equal distance to two atoms (Figure 24a). The preferential locations for the counterion around Nafion fragments are the same, but the overall range of possible locations is broader, and the cloud of preferential locations is smeared out (Figures 10a and 10d), in particular the counterion may be located in the center between all three oxygens, which is not seen in sPS solution.

Overall, the anisotropic structure around the phenylsulfonate group of sPS is much more pronounced than around the Nafion sidechain. Figure 24b shows preferential locations of OP oxygens in the first shell, which form six identifiable clouds corresponding to the six locations of the counterion. The preferential locations of the phosphorus atom and methyl group bound to phosphorus demonstrates a distinct orientation pattern, while the first solvation shells around Nafion, though very strong, are mostly isotropic (Figure 25).

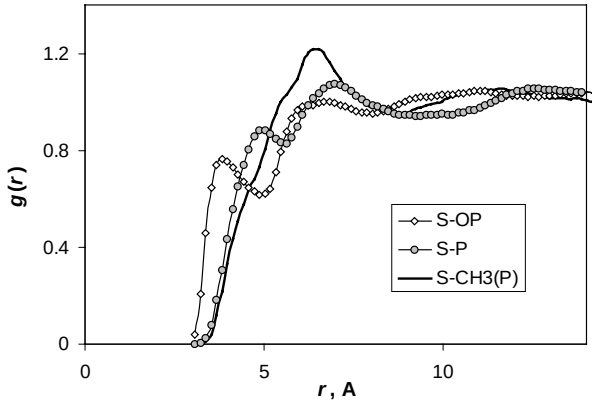

Figure 25. Radial distribution functions of counterions DMMP atoms around the sulfonate groups of sPS olygomers in DMMP-water 1:1 (vol) mixture. For atom denotations see Figure 15.

Solvation in water-DMMP binary mixture**.** As was shown in ref [3], the model Nafion sidechains introduced to DMMP-water binary solution, caused a segregation of the mixture into two subphases. A somewhat similar picture was observed in the solutions of sPS oligomers in the water-DMMP binary solvent. However, the segregation effect caused by the sPS oligomers was not that pronounced. DMMP surrounds the aliphatic backbone and the phenyl groups, while water mostly surrounds the sulfate groups and counterions. However, water cannot completely displace DMMP off the first solvation shell of both sulfate group and the anion. For example, Figure 25 shows that the first peak is still present on O_P-S RDF that indicates the presence of DMMP in the first solvatioin shell of the sulfonate group; in the second shell (distance of 6Å) the RDF is very close to 1, reflecting that the local composition of the second shell is the same as in the overall composition.

It should be noted that the hydrogen bonds between water and sulfonate groups in the mixture are more stable than in pure water, despite a mostly aqueous environment around the sidechains. We obtained the O_W-O_S residence time of 15.8ps, almost twice as long as for Nafion in pure water. The exact reason for this difference is unclear. It seems likely that larger and less mobile DMMP molecules surrounding the sulfonate groups solvated with waters constrict the motion of water and counterions making the water molecules less mobile.

IV. 5. Discussion.

We have performed a molecular dynamics simulation studie of sulfonated polystyrene fragments in water, nerve agent simulant dimethylmethylphosphonate, and their binary mixture in pursuit for a better understanding of interactions and dynamics in the hydrophilic subphase of solvated triblock copolymer membranes. We have established the forcefield parameters related to the sulfonate group by using ab initio optimization with the restricted Hartree-Fock method. We compare the specifics of solvation of sPS and Nafion.

We found a significant deplastification effect of DMMP both on sPS and Nafion polymer: the flexibility of the polymer backbone in DMMP and DMMP-water binary mixture is

substantially reduced compared to the backbone flexibility in pure water. A deplastification effect was also observed when single-valent potassium or two-valent calcium cation were replaced by tri-valent aluminum cation. The strong electrostatic forces in the last case cause strong conformation changes in sPS.

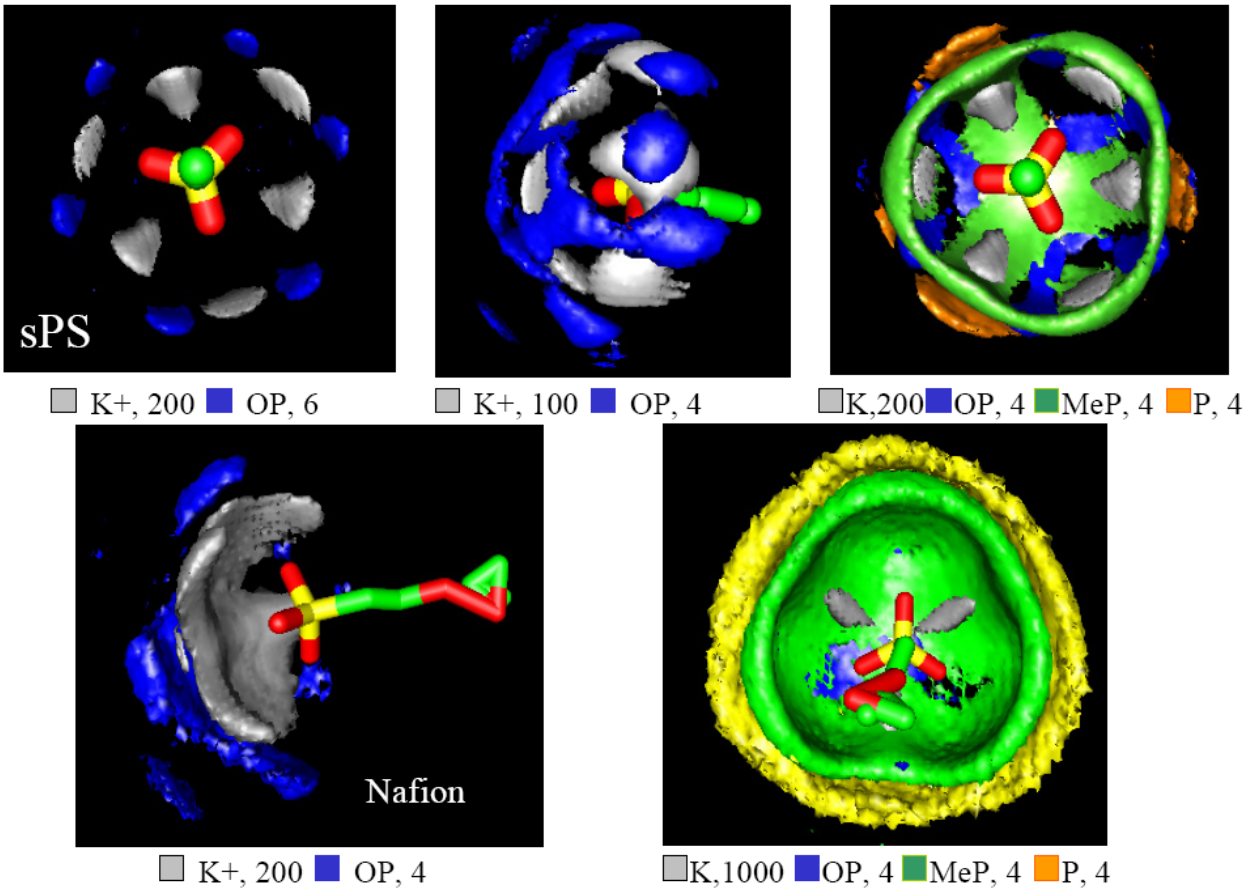

Figure 24 Spatial distribution functions of K+ counterions and DMMP atoms (for denotations see Figure 15) around the sulfonate group of sPS (top) and Nafion (bottom). The sticks show the position of the atoms of phenyl group averaged in a coordinate system rigidly attached to two of S-O vectors. Different colors correspond to different atoms indicated under each image. The numbers are the relative intensities, i.e. the colored clouds show the areas where the average local concentration of certain atom is higher than the average multiplied by the intensity level

The solvent structuring around the sulfonate groups of sPS for both water and DMMP is similar to that of Nafion but shows a much greater anisotropy. The solvation shell of water around the sulfonate group is determined by hydrogen bonding between water and the sulfonate group oxygens. Despite apparent similarity in numbers and lifetimes of the hydrogen bonds, the spatial distribution functions show distinct anisotropic structuring in the first solvation shell around the sulfonate groups in both water and DMMP, which is not observed in Nafion. We relate this changes to the lack of flexibility of the phenylsulfonate group (as compared to the Nafion sidechain) and anisotropy of the phenyl ring.

The simulation of sPS fragments in the water-DMMP binary mixture showed a partial segregation of the solvent mixture with DMMP prevailing around the hydrocarbon backbone and water surrounding the sulfonate groups. Both water and DMMP were found in the first solvation

shell of the counterion. The segregation is less pronounced in sPS than in Nafion, likely because of a smaller flexibility of the backbone and a shorter distance between the sulfonate groups in sPS. We expect that the hydrophilic subphase of the sulfonated triblock copolymer membranes swollen in water and DMMP will remain uniform at the scales smaller than 30Å.

It is worth noting that the structural properties of sPS solutions obtained in this work can be employed for the development of a forcefield for mesoscale simulations of the hydrophilic phase of the triblock copolymer membranes using of the concept of the mean force potential. Fitting the distribution functions for the backbone conformations, we have derived a coarse-grained model of sPS with the effective bead representing four styrene monomers and obtained the potential of mean force sPS in water and DMMP. These results will be published elsewhere.

V. Large-scale molecular dynamics simulation of microstructure and molecular mobility of water and DMMP in sulfonated polystyrene.

V.1. Systems and methods. Sulfonated polystyrene was represented by short fragments (oligomers) of tactic PS composed of twenty monomers with some of them sulfonated in *para* position. We considered two sulfonation levels: 100% sulfonation (sulfonate groups were attached to all phenyl rings) and 40% sulfonation, with only 8 sulfonate groups per 20 phenyls (Figure 26 a,b). We also considered one model of random sPS-PE copolymer also depicted in Figure 26c. The counterion was Ca^{+}.

Table 4. Systems considered and their physical properties

Polymer *	Water, wt % §	DMMP, wt % §	D_{H2O} 10^{-9} m/s^2	D_{Ca++} 10^{-9} m/s^2	D_{DMMP} 10^{-9} m/s^2	n_{HB} ‡ H2O-H2O	n_{HB} ‡ H2O-DMMP	n_{HB} ‡ H2O-O3S	n_{HB} ‡ total
sPS, 40%	15		0.030	0.0008†		0.74		0.91	1.65
sPS, 40%	30		0.21	0.0045		1.17		0.66	1.83
sPS, 40%	54	0	0.91	0.035		1.47		0.49	1.96
sPS, 40%	54	10	0.58	0.019	0.035	0.96	0.03	0.50	1.49
sPS, 40%	54	50	0.36	0.0096	0.041	1.40	0.13	0.45	1.98
sPS, 40%	54	100	0.19	0.0078	0.052	1.30	0.25	0.45	1.95
sPS, 100%	15		0.012	0.0006†		0.28		1.16	1.44
sPS, 100%	50		0.067	0.0007†		0.86		0.94	1.8
sPS-PE, 100%	R		0.11	0.0022		0.36		0.95	X

* skeleton chemical structure and sulfonation level. See Figure 1.
§ ration of solvent weight to dry polymer weight
‡ donated per H_2O molecule; hydrogen bond between two oxygens is considered established if the distance between the oxygens is less than 3.4 Å and OHO angle exceeds 120deg
† counterion diffusion coefficients in some systems are difficult to evaluate for being too low

The simulation procedure was similar that employed in our previous works: the oligomers, counterions and solvent molecules were placed in a cubic box at very low density.

Then the system was shrunk in constant pressure MD simulation at T = 303K (maintained by simple velocity scaling) and pressure of 100atm. After the density of 0.9g/cm^3 was reached, the simulation proceeded at T = 303K and P = 1atm maintained with Nose-Hoover [66] thermostat. System equilibration proceeded for 2ns followed by additional 3.8 to 6 ns MD simulation over which system configuration was periodically saved to disc for analysis. We used standard Verlet algorithm with the timestep of 0.5fs during the system contraction and 2fs afterwards. Long-range electrostatic forces were calculated using Ewald summation. For sPS fragments, we employed second-order classical forcefield (Section IV). Water was presented by a rigid SPCE model [77] and the forcefield for DMMP was introduced by us in ref [3]

V.2. Nanostructure and dynamics of hydrated sPS: Dependence on hydration

In this section, we discuss nanostructure and dynamics of hydrated sPS with 40 % of sulfonation at water content of 15 to 54 % of the dry polymer weight. The limit of 54% was derived from the experimental data on water sorption in DAIS sulfonated PS-(PE-PB)-PS triblock copolymer membranes with the same counterion, assuming that water sorption in the hydrophobic phase is negligible [54]; 54 wt % of the sPS would correspond to water partial pressure of 90% of that of saturated water vapor at 298K, which is close to realistic conditions of membrane exploitations.

Because Nafion is the standard system of comparison in experiments and simulation alike, it makes sense to evaluate the relative volumes of projected hydrophilic and hydrophobic phases. Water content of 15 to 54 wt % approximately corresponds to 3 to 11 water molecules per sulfonate group, which is also typical for cation modified Nafion membranes. However, the relative volume of the hydrophilic subphase at full sulfonation in is much larger than in Nafion with standard equivalent weight of 1200D, because the volume occupied by the skeleton fragment containing one sulfonate group in sPS at 40% sulfonation is nearly 2 times smaller than the monomer volume of Nafion. This will apparently cause substantial shift in nanostructure and dynamics compared to Nafion and other perfluorinated systems considered in previous simulations.

Another feature specific to this simulation work is the double charge counterion, which obviously influences the system structure, since two sulfonate groups are needed to neutralize one ion of calcium. Figure 27a shows radial distribution functions between the sulfur atoms in hydrated sPS at different hydration levels. At all hydration levels, these RDFs show distinct correlations at distances up to 15 Å. These correlations are similar at all hydration levels, although the relative significance of different peaks changes as hydration increases.

The correlations reveal the existence of typical patterns of mutual arrangements of sulfonate groups in the hydrated polymer. Figure 27b that exhibits the intramolecular RDFs for the same systems, shows that the peaks for the total and intramolecular RFDs do not coincide. Therefore, the typical patterns of the sulfonate groups arrangement are not caused by the predominant conformations of individual polymer chains. The first peak of the overall RDFs at about 4.6Å may only correspond to a configuration where two sulfonate groups are “jammed together” and neutralized by one counterion. As hydration increases, such configurations lose importance, as this peak on the RDF disappears. In another typical configuration, two sulfonate groups are essentially tied together by the counterion located in the palms of both sulfonates (this corresponds to the second peak on the RDF at 7.4Å on Figure 27a; the exact distances should be taken with a grain of salt, since LJ models cannot describe dissociation in the systems of this type, but we believe that the general picture is correct). At higher hydration, their contribution

decreases, but remains significant. However, the fractions of fully hydrated calcium ions (completely surrounded by water and essentially detached from particular sulfonate anions) are low and do not exceed 10% even at maximum hydration. This means that effectively hydration causes dissociation of $(\text{-RSO}_3)_2\text{Ca}$ quadrupole into $(\text{-RSO}_3\text{Ca})^+$ and $(\text{-RSO}_3)^-$ ion pair with each of the ions covalently attached to the skeleton. The solvation of this system must therefore differ from that described in section IV.

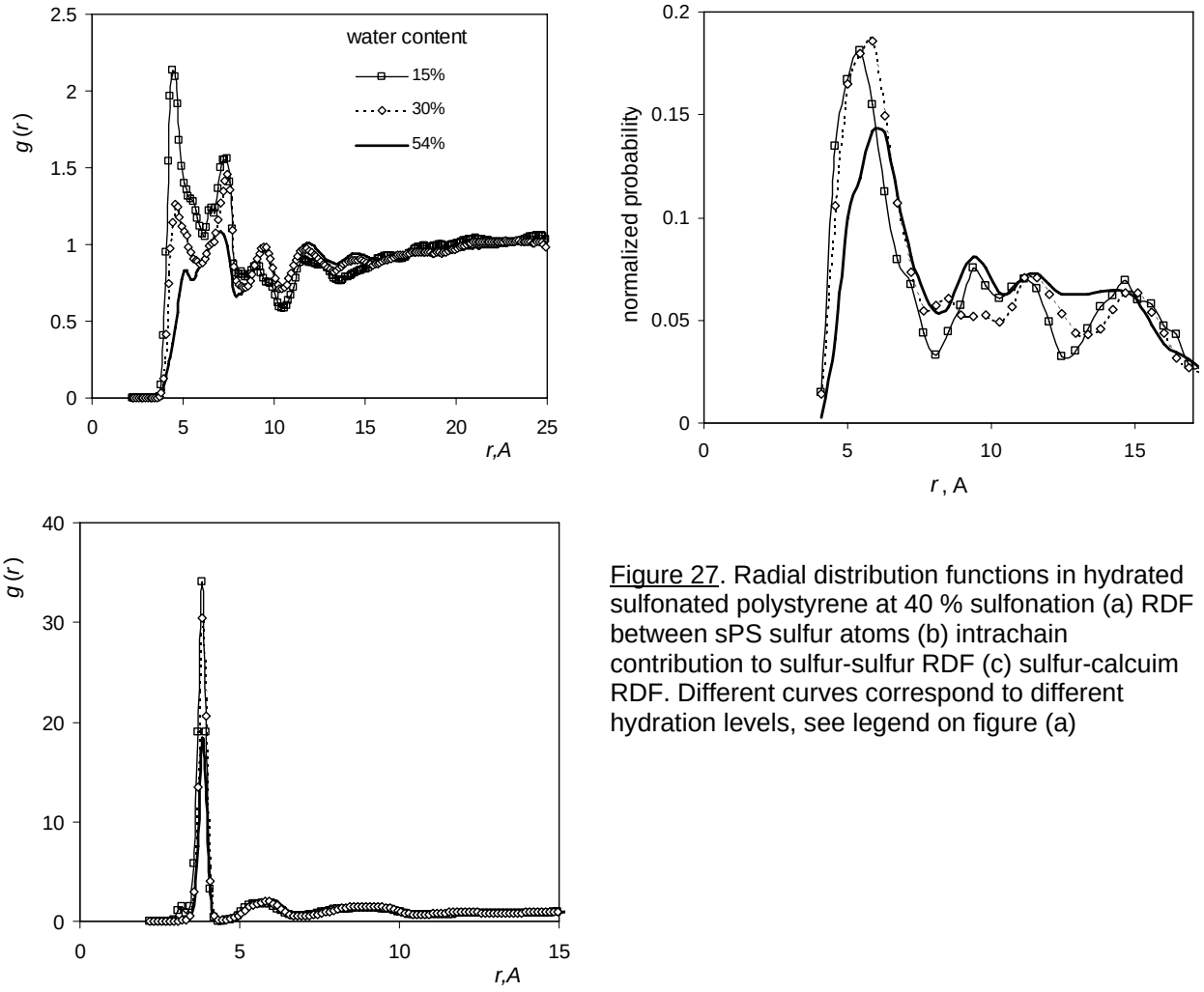

Figure 27. Radial distribution functions in hydrated sulfonated polystyrene at 40 % sulfonation (a) RDF between sPS sulfur atoms (b) intrachain contribution to sulfur-sulfur RDF (c) sulfur-calcuim RDF. Different curves correspond to different hydration levels, see legend on figure (a)

The nanostructure of the membranes was characterized in terms of solvent cluster sizes and hydrogen bonding, which was tracked using geometric criteria ([2, 39], see Table 4). Two water molecules were considered as belonging to the same water cluster if the distance between the oxygens was lower than 4.5Å, which is the beginning of the second maximum on the RDF for pure liquid. At 15% water content, about 30% of all water molecules formed small (<4 molecules) disconnected clusters, but the majority aggregated into connected channels of approximately cylindrical shape, even though the channels didn't span through the system (Figure 28a). Despite the continuity of the cluster, geometric analysis shows that in average a water molecule donates 0.9 hydrogen bond to sulfonate group, (which means that practically every water molecule neighbors a sulfonate oxygen) and only 0.75 bond to another water. Thus,

the diffusion coefficient of water found from mean square displacement is two orders of magnitude lower than in the bulk liquid. It would become much lower if the simulation time increases due to the discontinuity of the hydrophilic phase.

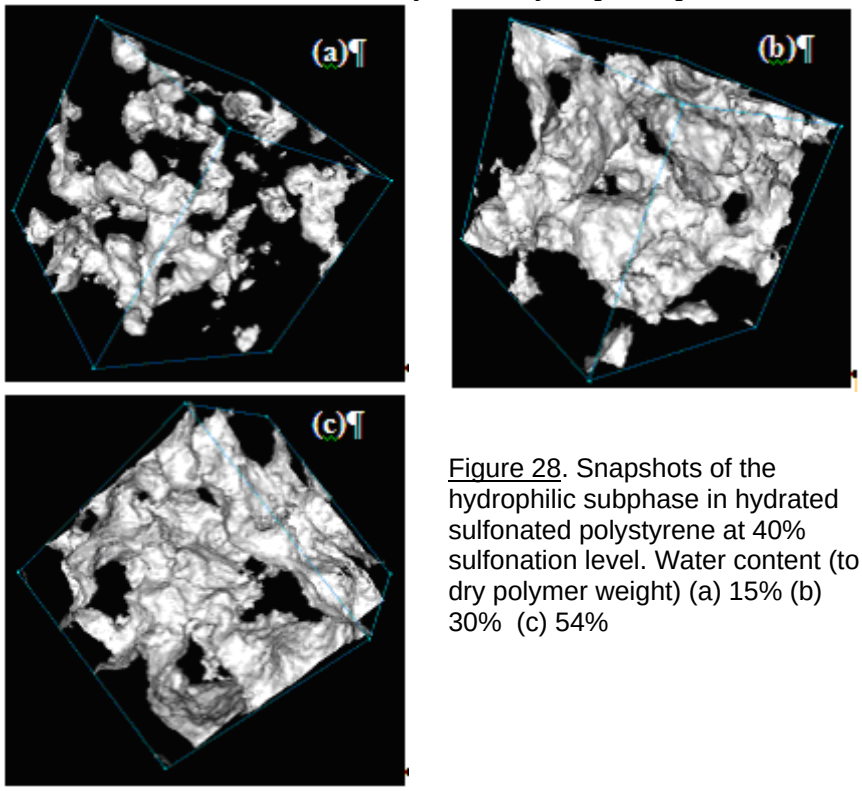

Figure 28. Snapshots of the hydrophilic subphase in hydrated sulfonated polystyrene at 40% sulfonation level. Water content (to dry polymer weight) (a) 15% (b) 30% (c) 54%

As hydration increases, the hydrophilic phase grows in volume and becomes continuous (Figure 3b,c). At maximum hydration, water diffusion coefficient raises to one third of that in liquid water, and counterion diffusion also becomes visible. Typical water molecule donates two hydrogen bonds, as in the liquid water. However, the segregation scale in not even close to that in Nafion, where clusters of 30Å and larger were reported from experiment and simulations alike at lower water content. At 54% wt of water, every other water molecule still donates a hydrogen bond to a sulfonate group, which means that the influence of the backbone on water structure is still very high.

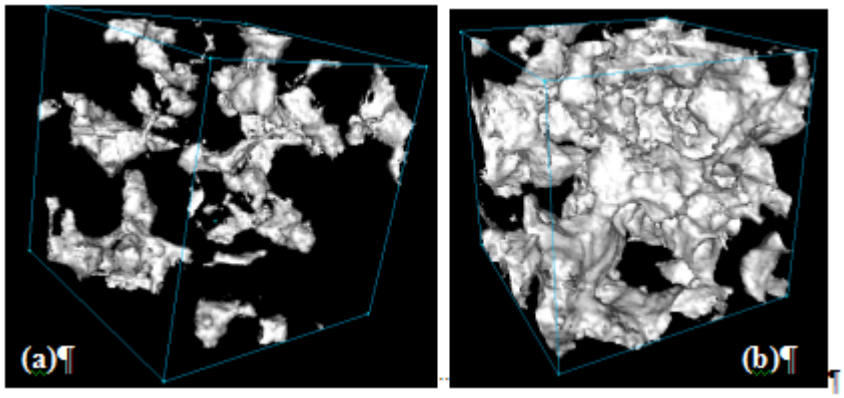

Figure 29 Hydrophilic subpphase of hydrated membranes: (a) Sulfonated polystyrene 100% sulfonatied at 15% wt water content (b) 1:1 ethylene-styrene copolymer 100% Sulfonated at 39% water content.

V.3. Nanostructure and dynamics of hydrated sPS: Dependence on the backbone structure and sulfonation

To reveal the influence of the sulfonation level, we considered the same systems (water content of 15 % wt and 54 % wt) at 100% polymer sulfonation. One has to keep in mind that the same relative water content at different sulfonation level corresponds to a different water activity. Therefore, it is more correct to consider the influence of the sulfonation at the same water activity. However, we did not find necessary data for cation substituted sPS in the literature, and the evaluation of the chemical potential of the solvent in segregated polymers via a simulation was beyond the abilities of the MD simulations. A cluster analysis shows that at 100% sulfonation, more water molecules reside in small clusters containing less than four molecules, and the hydrophilic subphase has more discontinuous inclusions (Figure 29a) resulting in a lower water diffusion coefficient and a much smaller number of water-to-water hydrogen bonds. From the comparison of diffusion coefficients for 100% sulfonated and 40% sulfonated samples, it arrears that at the same number of water molecules per sulfonate group, the diffusion is faster at 40% sulfonation level.

Hydration in pseudorandom copolymer (Figure 26c) was studied only at 100% sulfonation and 39% water content. This water content corresponds to 11 water molecules per sulfonate group; in this sense, or to 54% water sorption in sPS with 40% sulfonation level. The ratio of styrene to ethylene monomer numbers generally determines the volume of the polymer per one sulfonate group. The skeleton flexibility differs also, as the neighboring sulfonate groups on the same chain are separated by larger distances compared to sPS at the sulfonation levels below 100%.

Figure 29c shows that segregation exists in pseudorandom copolymer also. Water in this system forms a continuous subphase, and water diffusion is slightly slower than in the corresponding 40% sulfonated sPS. Similarly to the 40% to 100% sulfonation trend, this seems surprising because the relative volume of the hydrophilic subphase increases the random copolymer is larger than in 40% sPS. Thus, we have to conclude that the reduction of diffusivity reflects the dispersion of the hydrophilic subphase that is confirmed by the relative number of water-water and water-sulfonate hydrogen bonds.

V.4. Mobility of DMMP

In our sPS system with 40% sulfonation, we fixed water content at 54% and added DMMP, varying the content from 10% to 100% of the dry polymer weight. The upper limit of this range approximately corresponds to the maximum reported by Dr. Schneider (private communication). Solvation of sulfonate groups and counterions is demonstrated by RDFs shown in Figure 30a-c. Similarly to the water-only systems, most counterions are still associated with one sulfonate group. It is clear that the counterions are surrounded by both negatively charged water oxygens and the oxygens of DMMP bonded to the phosphorous atom. While there is a slight preference to water, DMMP is not overwhelmed in the first solvation shell. On S-O and S-P RDFS (Figure 30b) where all sulfonate groups count, we observe a high first peak corresponding to water molecules that form hydrogen bonds to the sulfonate groups. This peak is naturally absent for DMMP but it is clear than we cannot say that the sulfonate groups are immersed in water as it was observed for large quantities of solvents. Our observation confirms the hypothesis made by Drs. Rivin and Schneider, RDEC, about a competition of water and DMMP for the solvation of sulfonate groups in sPS, which was not observed in Nafion [11]. On

the other hand, the RDFs between the phosphorous and benzene ring atoms (Figure 30b) undoubtedly show us that DMMP is predominant around the skeleton.

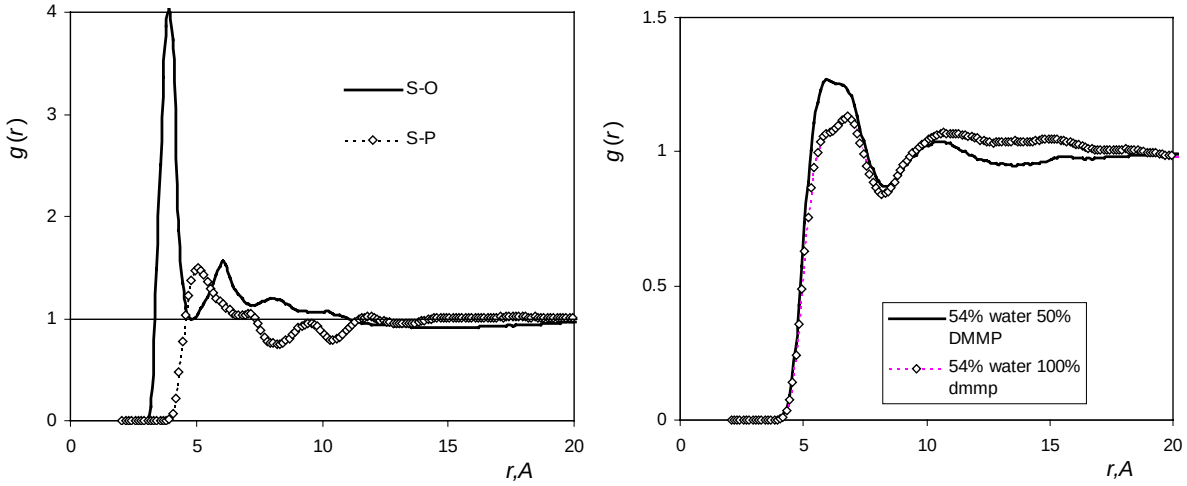

Figure 30. Radial distribution functions for 40% Sulfonated sPS-water-DMMP system (a) sulfur-water oxygen RDF for 54% water, 50% DMMP content (b) RDF between the root benzene carbon (the one attach to the aliphatic chain) and phosphorous of DMMP at different DMMP content

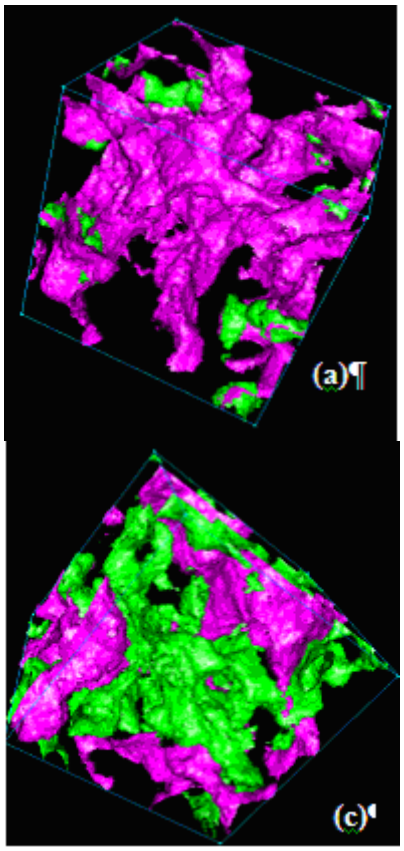

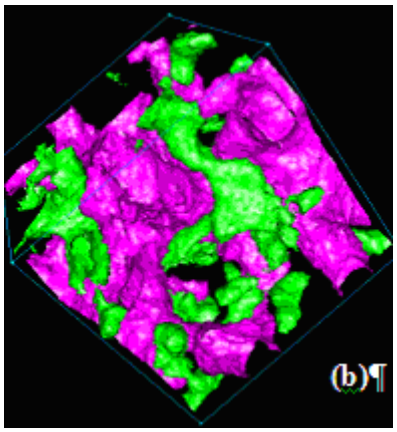

Figure 31. Snapshot of areas occupied by water (purple) and DMMP (green) sorbed in 40% sulfonated sPS (a) 54% of water (to dry polymer weight) 10% of DMMP; (b) 54% of water, 50% of DMMP (c) 54% of water, 100% of DMMP

Cluster analysis of the sPS-water-DMMP samples shows that in all systems, the mobile species (water, DMMP, ions considered together) form a single continuous subphase. However, at higher DMMP concentrations (50 and 100 wt %), DMMP was found to form a continuous subphase on

its own. In fact, the diffusion coefficient of water steadily goes down with the increase in DMMP content (and DMMP diffusion coefficient), despite the obvious increase in the cumulative volume of the mobile subphase(s), serving a good indication that water and DMMP have separate pathways through the system. Also, in a contrast to the bulk solution, where DMMP was found to accept 15-2 hydrogen bonds from water molecules in average [3], which is on par with water molecule itself, here each molecule only accepts 0.75 hydrogen bonds in average at 50% and 100% wt DMMP content, compared to 1.3-1.4 bond accepted by water.

The nanosegregation in this system is shown in Figure 31, which shows the evolution of the nanostructure as the DMMP is added. It confirms that water and DMMP form two irregular suphases with high contact surface.

V.5. Discussion

Using classical molecular dynamics simulations, we explored nanostructure and diffusion of water and DMMP in the hydrophilic subphase of sulfonated polystyrene-polyolefin block copolymer membranes. sPS fragments with different degree of sulfonation with calcium counterions were explored at different composition water-DMMP mixture. We found that sulfonated sPS upon hydration is strongly inhomogeneous: similarly to the Nafion case, one could identify hydrophilic subphase (water) and hydrophobic subphase formed by the aliphatic skeleton and benzene rings, in particular the non-sulfonated ones. The segregation scale is much smaller than that in Nafion. As sulfonation increases, the hydrated polymer becomes more homogeneous and water diffusion slows down.

With both water and DMMP present in the system, the diffusion coefficients of DMMP compared to those of water turned out to be rather high even at DMMP content well below the maximum. This fact is rather discouraging and signals for chemical modifications of the material. From our simulation we derived that DMMP forms its own subphase and its pathways through the polymer differ from those of water.

VI. Morphology of sulfonated triblock-copolymer membranes

VI.1. Mesoscale Model.

Mesoscale simulation methods such as DPD [83] or Mesodyn were developed for fluid systems. In nanostructured SEBS considered here, the length of the blocks and segregation scale are sufficient for the polymers to be considered as “glassy”. However, water and DMMP inevitably plasticize the polymer, especially the high-melting PS part. In our opinion, SEBS copolymer melt at T = 473K is a reasonable systems to consider as a precursor to solvated SEBS membranes at room temperature.

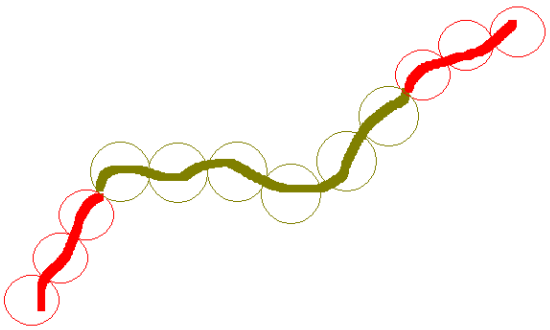

Figure 32. Schematic representation of block copolymer with beads of two different types

As usual in mesoscale simulations, the polymers were presented as sequences of beads. Different blocks were represented by different bead types (Figure 32). In each simulation, we had two bead types (for middle and end blocks). Since the polymer molecular weight was fairly high, yet each chain should be presented with minimal number of beads, we decided to use different bead size and parameters for each system.

Standard for DPD simulations soft interaction potential $F_{ij} = a_{ij} (1 - r_{ij})$ (where F is the force and r is the distance between the beads, and a is the conservative potential parameter for the particular bead types) was employed to describe interactions between the beads. The neighboring beads were connected by harmonic bonds of one bead diameter in length. No chain rigidity potential was imposed, for bead size exceeded the correlation length.

Table 5 **Triblock Polymer Composition**

	Kraton polymers		Used by Don Rivin	Aldrich polymers	
	K64	K69	SEBS	Lo Mw *	Hi Mw
Polymer mol weight	125000	109000	49000	89000	118000
Total styrene content	64	69	66	29	28
End block conc., wt%	29	38	66	29	28
End block mol weight	18100	20600	16170	12905	16520
Weight mid block/end block	2.45	1.65	0.52	2.45	2.57
Soft segment mol weight	88800	67800	16660	63190	84960
Weight styrene/butadiene	0.97	1.01	0	0	0
sulfonation level	0.39	0.39	0	0	0
mols sulfonated/ g polymer	2.40E-03	2.59E-03			
mol wt sulfonic acid	80	80			
additional weight	0.192	0.207			
IEC meq/g	2.013	2.144			
number density ρ*	3	3	3	3	3
m (monomers in 1 bead, endblck)	65	65	60	60	60
N (beads in endblock)	2.06	2.34	2.59	2.07	2.65
N (beads in endblock -- exact integer)	2	2	3	3	3
linear system size, nm	122	128	106	98	107
resulting morphology	cylindrical hexagonal	cylindrical hexagonal	lamellae	lamellae	lamellae
effective period, nm	20.4	22.7	16.6	16.6	18.0
radius of hydrophilic formation, nm	8.3	11.2	10.0	5.8	6.3

Table 5 gives the systems considered and models chosen. Mesoscale simulations of polystyrene containing systems have been described in the literature . Because the natural chain rigidity is very close for sulfonated and non-sulfonated PS, we assumed that the ratio of

conservative parameters for the two polymers is equal to the ratio of compressibilities of sulfonated and non-sulfonated 2,4,6-triphenylhexane. The ratio was obtained from two independent molecular dynamics simulations at the same temperature of T = 473K. For Kraton copolymers, which contains styrene in the midblock, the conservative parameter was obtained as a linear combination of those for homopolymers, proportional to the weight fraction of each monomer. Using data of ref [84], this leads us to a=74 for PS beads.

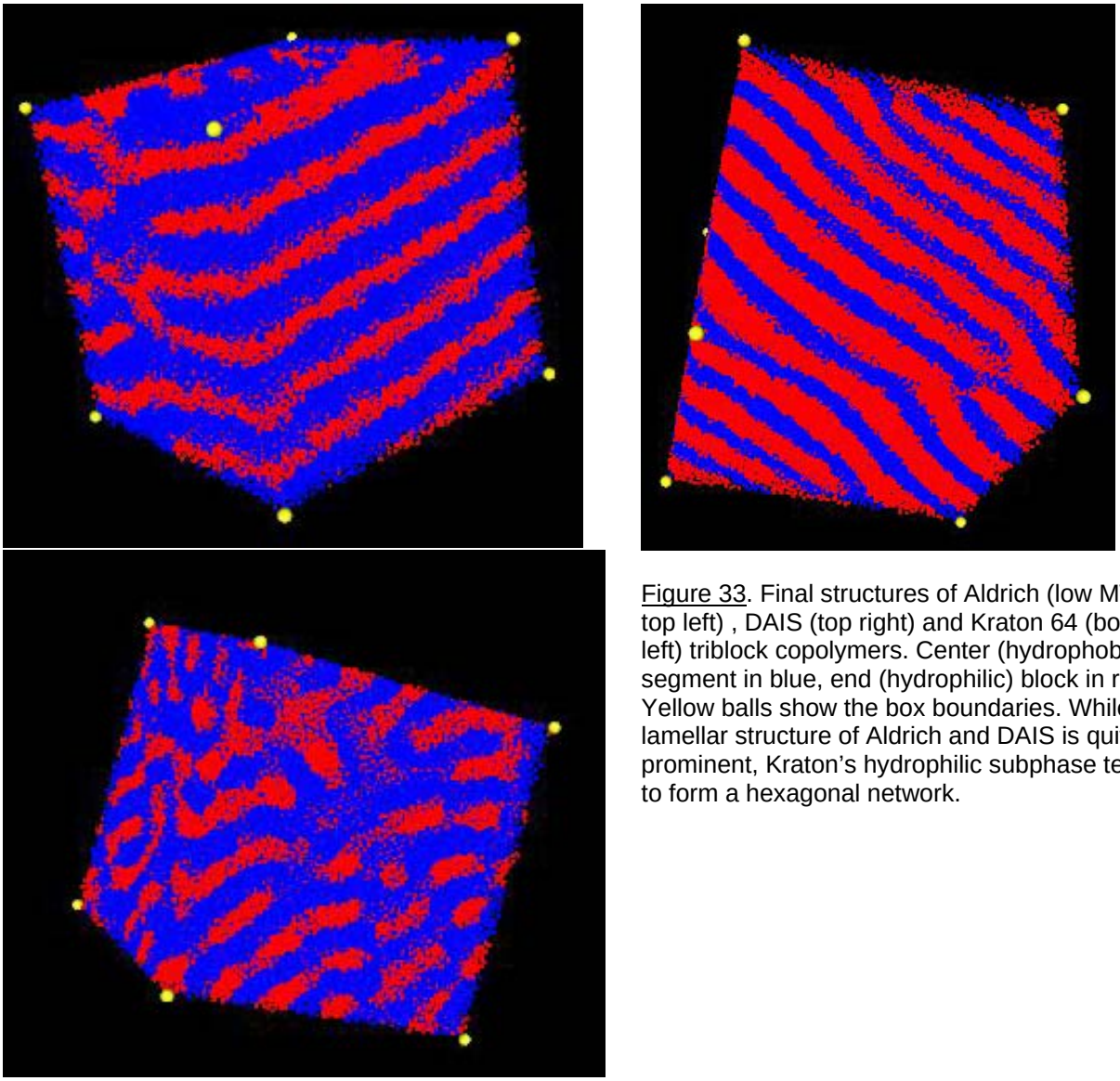

Figure 33. Final structures of Aldrich (low MW, top left) , DAIS (top right) and Kraton 64 (bottom left) triblock copolymers. Center (hydrophobic) segment in blue, end (hydrophilic) block in red. Yellow balls show the box boundaries. While lamellar structure of Aldrich and DAIS is quite prominent, Kraton's hydrophilic subphase tends to form a hexagonal network.

The parameter for interactions between the beads of different types was mapped onto Flory-Huggins coefficient derived in ref [52] from experimental data. Ref 17 shows that the unlike parameter depends linearly on the Flory parameter at $\rho^* = 3$: $\chi N = 0.286\Delta a$, where $\Delta a = a_{\text{PS-PS}} - a_{\text{PS-PB}}$. From $\chi = 0.24$ for SEBS, obtained in ref [52] we get $\Delta a = 34.48$. The parameter for Kraton simulations was scaled proportional to the styrene content.

All our simulations were carried out T = 473K, with time step of 0.04, which corresponds to approximately $2*10^{-10}$s for these systems. From $4*10^5$ to $2.4*10^6$ steps were done for different systems; the longest simulation equals to nearly a microsecond. The system size was close to 0.1μm (Table 5).

The DAIS and Aldrich systems easily come to equilibrium lamellae structures (Figure 33a,b). Kraton melts turned out to be pretty stubborn, but clearly indicated a tendency to cylindrical mesophases (Figure 33c). For Kraton-69, the equilibrium was not reached and after nearly a millisecond simulation, the structure was still disordered, although a tendency to cylindrical morphology was quite pronounced.

VI.2. Discussion.

We explored the morphologies of sSEBS triblock copolymer membranes considered by RDEC researchers for experimental studies. These polymers differ by the weights of different blocks and composition of the hydrophobic blocks. Our DPD simulations show strong segregation into mostly regular phases; DA block copolymers tent to segregate into lamellae morphologies, while Kraton samples with longer middle blocks showed preference to hexagonal morphologies with cylindrical hydrophilic aggregates. These two morphologies were also observed for other triblock copolymers of sPS with polyolefins in the literature [52, 85]

VII. Summary of the project results and suggestions for further studies.

Concentrating on sulfonated polystyrene containing block-copolymers, we developed a hierarchical multiscale methodology for computational studies of the membrane morphology at environmental conditions, and the membrane sorption and transport properties with respect to water and nerve gas simulant dimethylmethylphosphonate (DMMP). The hierarchical approach implies that the results of simulations on a lower scale level in conjunction with available experimental data serve as input parameters for simulations on the upper scale level. The methods developed include: a) quantum mechanical *ab-initio* calculations of specific interactions of DMMP and water with the membrane fragments, b) atomistic molecular dynamic simulations of membrane solvation in water-DPPM mixture with different counterions, c) large-scale molecular dynamic simulations of membrane segregation and mobilities of chemicals, and d) dissipative particle dynamics simulations of mesoscopic morphologies in solvated membranes of different composition. This scheme allows us to explore the systems of interest in wide range of length- and timescales, from individual molecules and femtoseconds to mesoscale morphology of characteristic size of tens of nanometers and microseconds. We explored the molecular mechanisms of sorption and mobility of DMMP in the membranes and studied their dependence on the membrane composition and the degree of sulfonation, the hydration level, and the type of the counterion. The results of simulations of triblock copolymers were compared with the properties of Nafion studied earlier. The molecular simulation studies were performed in concert with the experimental work at Natick Soldier RDEC, Natick, Ma. The systems for simulations were recommended by RDEC researchers, and the simulation results were compared with RDEC experimental data.

The results of the simulation study revealed the following specific features of interaction of DMMP with sulfonated triblock copolymers:

- The interaction of DMMP with the phenylsulfonate groups in hydrated polystyrene differs substantially from the interaction of DMMP with the sidechains in hydrated Nafion. While in Nafion, water and DMMP attack different groups, in sPS they tend to compete for the first solvation shell of the sulfonate anion. Real phosphor-organic CWA are expected to behave similarly. This is a promising sign because the competition with water reduces sorption and slows diffusion of organic chemicals.
- The counterion influences sorption and diffusion by affecting the interaction between the sulfonate groups and their solvation by the solvent, thus changing the conformation of the skeleton. Specific interactions of multivalent cations with DMMP are still unclear and need further studies
- The hydrophilic subphase of hydrated sPS is inhomogeneous and segregates onto irregular domains formed by water and hydrophobic groups respectively. The hydrophilic aggregates are cylindrical in shape at a low water content and become completely irregular at a higher water content. Even at the maximum uptake, the size of water aggregate does not exceed 2nm. The system becomes more homogeneous at a higher sulfonation level; therewith, water diffusion slows down.
- The diffusion coefficient of DMMP in the hydrophilic subphase is relatively high compared to that of water that calls for the further search for a more suitable chemical structure of PEM. It appears that the pathways of DMMP and water diffusion through the sPS subphase are different.
- On the membrane scale, the polymer exhibits strong segregation into hydrophilic and hydrophobic subphases; the predicated segregation morphology is lamellar in DAIS and Dow triblock copolymers and hexagonal, with cylindrical hydrophilic channels, in Kraton copolymers,

The computational methods developed can be further advanced and employed for molecular design of novel protective materials and predictions of the membrane permeability and blocking efficiency with respect to real CWA, such as nerve and vesicant agents, including GB (sarin), HD (sulfur mustard), and others. Moreover, there is increasing need for improved barrier materials to protect personnel from toxic chemical exposure, and the Army is facing new challenges with risks of terrorist attacks, which may involve non-traditional chemicals sourced through the industrial sector or produced by other means. The simulation methods developed in this project can be instrumental in performing virtual experiments with traditional CWA and various toxic industrial chemicals (TIC), which cannot be readily explored experimentally that will guide the materials scientists and will help rationalize expensive and time-consuming experimentation. There is a lot of interest in assessing how well CWA simulants, like dimethylmethylphosphonate (DMMP), can be substituted for real agents in experimental studies. The molecular simulation methods will help select most suitable candidate materials for experimental validation, providing a better understanding of physical and chemical mechanisms of interactions of toxic agents and simulants with barrier materials. Predictive capabilities of the multiscale simulation models will lead to specific suggestions on structural/chemical modifications of barrier nanomaterials and improvement of their properties for better CWA and TIC protection.

Literature

1. Serpico, J.M., et al., *Transport and structural studies of sulfonated styrene-ethylene copolymer membranes.* Macromolecules, 2002. **35**(15): p. 5916-5921.
2. Vishnyakov, A. and A.V. Neimark, *Molecular simulation study of Nafion membrane solvation in water and methanol.* Journal of Physical Chemistry B, 2000. **104**(18): p. 4471-4478.
3. Vishnyakov, A. and A.V. Neimark, *Molecular model of dimethylmethylphosphonate and its interactions with water.* Journal of Physical Chemistry A, 2004. **108**(8): p. 1435-1439.
4. Jang, S.S. and W.A. Goddard, *Structures and transport properties of hydrated water-soluble dendrimer-grafted polymer membranes for application to polymer electrolyte membrane fuel cells: Classical molecular dynamics approach.* Journal of Physical Chemistry C, 2007. **111**(6): p. 2759-2769.
5. Paddison, S.J., L.R. Pratt, and T.A. Zawodzinski, *Conformations of perfluoroether sulfonic acid side chains for the modeling of Nafion (R).* Journal of New Materials for Electrochemical Systems, 1999. **2**(3): p. 183-188.
6. Paddison, S.J. and T.A. Zawodzinski, *Molecular modeling of the pendant chain in Nafion (R).* Solid State Ionics, 1998. **115**: p. 333-340.
7. Urata, S., et al., *Intermolecular interaction between the pendant chain of perfluorinated ionomer and methanol.* Journal of Fluorine Chemistry, 2005. **126**(9-10): p. 1312-1320.
8. Urata, S., et al., *Intermolecular interaction between the pendant chain of perfluorinated ionomer and water.* Physical Chemistry Chemical Physics, 2004. **6**(13): p. 3325-3332.
9. Urata, S., et al., *Molecular dynamics simulation of swollen membrane of perfluorinated ionomer.* Journal of Physical Chemistry B, 2005. **109**(9): p. 4269-4278.
10. Vishnyakov, A. and A.V. Neimark, *Molecular dynamics simulation of nafion oligomer solvation in equimolar methanol-water mixture.* Journal of Physical Chemistry B, 2001. **105**(32): p. 7830-7834.
11. Rivin, D., et al., *Simultaneous transport of water and organic molecules through polyelectrolyte membranes.* Journal of Physical Chemistry B, 2004. **108**(26): p. 8900-8909.
12. Cui, S.T., et al., *A molecular dynamics study of a nafion polyelectrolyte membrane and the aqueous phase structure for proton transport.* Journal of Physical Chemistry B, 2007. **111**(9): p. 2208-2218.
13. Yamamoto, S. and S.A. Hyodo, *A computer simulation study of the mesoscopic structure of the polyelectrolyte membrane Nafion.* Polymer Journal, 2003. **35**(6): p. 519-527.
14. Vishnyakov, A. and A.V. Neimark, *Molecular dynamics simulation of microstructure and molecular mobilities in swollen Nafion membranes.* Journal of Physical Chemistry B, 2001. **105**(39): p. 9586-9594.
15. Spohr, E., *Molecular dynamics simulations of proton transfer in a model Nafion pore.* Molecular Simulation, 2004. **30**(2-3): p. 107-115.
16. Seeliger, D., C. Hartnig, and E. Spohr, *Aqueous pore structure and proton dynamics in solvated Nafion membranes.* Electrochimica Acta, 2005. **50**(21): p. 4234-4240.
17. Meier, F. and G. Eigenberger, *Transport parameters for the modelling of water transport in ionomer membranes for PEM-fuel cells.* Electrochimica Acta, 2004. **49**(11): p. 1731-1742.

18. Li, T., A. Wlaschin, and P.B. Balbuena, *Theoretical studies of proton transfer in water and model polymer electrolyte systems.* Industrial & Engineering Chemistry Research, 2001. **40**(22): p. 4789-4800.
19. Jang, S.S., et al., *Nanophase-segregation and transport in Nafion 117 from molecular dynamics simulations: Effect of monomeric sequence.* Journal of Physical Chemistry B, 2004. **108**(10): p. 3149-3157.
20. Jang, S.S., et al., *Nanophase segregation and water dynamics in the dendrion diblock copolymer formed from the Frechet polyaryl ethereal dendrimer and linear PTFE.* Journal of Physical Chemistry B, 2005. **109**(20): p. 10154-10167.
21. Elliott, J.A., et al., *Atomistic simulation and molecular dynamics of model systems for perfluorinated ionomer membranes.* Physical Chemistry Chemical Physics, 1999. **1**(20): p. 4855-4863.
22. Choi, P., N.H. Jalani, and R. Datta, *Thermodynamics and proton transport in Nafion - II. Proton diffusion mechanisms and conductivity.* Journal of the Electrochemical Society, 2005. **152**(3): p. E123-E130.
23. Blake, N.P., et al., *Structure of hydrated Na-Nafion polymer membranes.* Journal of Physical Chemistry B, 2005. **109**(51): p. 24244-24253.
24. Blake, N.P., G. Mills, and H. Metiu, *Dynamics of H2O and Na+ in nafion membranes.* Journal of Physical Chemistry B, 2007. **111**(10): p. 2490-2494.
25. Ayyagari, C., D. Bedrov, and G.D. Smith, *A molecular dynamics simulation study of the influence of free surfaces on the morphology of self-associating polymers.* Polymer, 2004. **45**(13): p. 4549-4558.
26. Urata, S., et al., *Molecular dynamics study of the methanol effect on the membrane morphology of perfluorosulfonic ionomers.* Journal of Physical Chemistry B, 2005. **109**(36): p. 17274-17280.
27. Commer, P., et al., *Modeling of proton transfer in polymer electrolyte membranes on different time and length scales.* Molecular Simulation, 2004. **30**(11-12): p. 755-763.
28. Dokmaisrijan, S. and E. Spohr, *MD simulations of proton transport along a model Nafion surface decorated with sulfonate groups.* Journal of Molecular Liquids, 2006. **129**(1-2): p. 92-100.
29. Spohr, E., P. Commer, and A.A. Kornyshev, *Enhancing proton mobility in polymer electrolyte membranes: Lessons from molecular dynamics simulations.* Journal of Physical Chemistry B, 2002. **106**(41): p. 10560-10569.
30. Roudgar, A., S.P. Narasimachary, and M. Eikerling, *Hydrated arrays of acidic surface groups as model systems for interfacial structure and mechanisms in PEMs.* Journal of Physical Chemistry B, 2006. **110**(41): p. 20469-20477.
31. Lamas, E.J. and P.B. Albuena, *Molecular dynamics studies of a model polymer-catalyst-carbon interface.* Electrochimica Acta, 2006. **51**(26): p. 5904-5911.
32. Petersen, M.K., et al., *Excess proton solvation and delocalization in a hydrophilic pocket of the proton conducting polymer membrane narion.* Journal of Physical Chemistry B, 2005. **109**(9): p. 3727-3730.
33. Paddison, S.J., *Proton conduction mechanisms at low degrees of hydration in sulfonic acid-based polymer electrolyte membranes.* Annual Review of Materials Research, 2003. **33**: p. 289-319.
34. Weber, A.Z. and J. Newman, *Modeling transport in polymer-electrolyte fuel cells.* Chemical Reviews, 2004. **104**(10): p. 4679-4726.

35. Gierke, T.D. and W.Y. Hsu, *The Cluster-Network Model of Ion Clustering in Perfluorosulfonated Membranes.* Acs Symposium Series, 1982. **180**: p. 283-307.
36. Gierke, T.D., G.E. Munn, and F.C. Wilson, *The Morphology in Nafion Perfluorinated Membrane Products, as Determined by Wide-Angle and Small-Angle X-Ray Studies.* Journal of Polymer Science Part B-Polymer Physics, 1981. **19**(11): p. 1687-1704.
37. Eikerling, M., A.A. Kornyshev, and U. Stimming, *Electrophysical properties of polymer electrolyte membranes: A random network model.* Journal of Physical Chemistry B, 1997. **101**(50): p. 10807-10820.
38. Ennari, J., M. Elomaa, and F. Sundholm, *Modelling a polyelectrolyte system in water to estimate the ion-conductivity.* Polymer, 1999. **40**(18): p. 5035-5041.
39. Lyubartsev, A.P. and A. Laaksonen, *Molecular Dynamics Simulations of DNA in Solution with Different Counterions.* J. Biomol.Struct. and Dyn, 1998. **16**: p. 579-587.
40. Duca, J.S. and A.J. Hopfinger, *Molecular modeling of polymers 18. Molecular dynamics simulation of poly(acrylic acid) copolymer analogs. Capture of calcium ions as a function of monomer structure, sequence and flexibility.* Computational and Theoretical Polymer Science, 1999. **9**(3-4): p. 227-244.
41. Groot, R.D., *Electrostatic interactions in dissipative particle dynamics-simulation of polyelectrolytes and anionic surfactants.* Journal of Chemical Physics, 2003. **118**(24): p. 11265-11277.
42. Wescott, J.T., et al., *Mesoscale simulation of morphology in hydrated perfluorosulfonic acid membranes.* Journal of Chemical Physics, 2006. **124**(13).
43. Galperin, D.Y. and A.R. Khokhlov, *Mesoscopic morphology of proton-conducting polyelectrolyte membranes of Nafion((R)) type: A self-consistent mean field simulation.* Macromolecular Theory and Simulations, 2006. **15**(2): p. 137-146.
44. Galperin, D.Y. and A.R. Khokhlov, *Mesoscopic Morphology of Proton-Conducting Polyelectrolyte Membranes of Nafion1 Type: A Self-Consistent Mean Field Simulation.* Macromolecular Theory and Simulations, 2006. **15**: p. 137-146.
45. Khalatur, P.G., S.K. Talitskikh, and A.R. Khokhlov, *Structural organization of water-containing Nafion: The integral equation theory.* Macromolecular Theory and Simulations, 2002. **11**(5): p. 566-586.
46. Mologin, D.A., P.G. Khalatur, and A.R. Kholhlov, *Structural organization of water-containing Nafion: A cellular-automaton-based simulation.* Macromolecular Theory and Simulations, 2002. **11**(5): p. 587-607.
47. Urakami, N. and M. Takasu, *The distribution of the gyration radius of a model of ionomer studied by multicanonical Monte Carlo simulation.* Molecular Simulation, 1997. **19**(1): p. 63-73.
48. Korolev, N., et al., *A molecular dynamics simulation study of oriented DNA with polyamine and sodium counterions: diffusion and averaged binding of water and cations.* Nucleic Acids Research, 2003. **31**(20): p. 5971-5981.
49. Korolev, N., A.P. Lyubartsev, and L. Nordenskiold, *Application of the Poisson Boltzmann polyelectrolyte model for analysis of equilibria between single-, double-, and triple-stranded polynucleotides in the presence of K+, Na+, and Mg2+ ions.* Journal of Biomolecular Structure & Dynamics, 2002. **20**(2): p. 275-290.
50. Lu, X.Y., W.P. Steckle, and R.A. Weiss, *MORPHOLOGY AND PHASE-BEHAVIOR OF BLENDS OF A STYRENIC BLOCK-COPOLYMER IONOMER AND POLY(CAPROLACTONE)*

Macromolecules, 1993. **26**: p. 3615.
51. Rivin, D. and N.S. Schneider. 2005.
52. Kim, B., J. Kim, and B. Jung, *Morphology and transport properties of protons and methanol through partially sulfonated block copolymers.* Journal of Membrane Science, 2005. **250**(1-2): p. 175-182.
53. Gromadzki, D., et al., *Morphological studies and ionic transport properties of partially sulfonated diblock copolymers.* European Polymer Journal, 2006. **42**(10): p. 2486-2496.
54. Schneider, N.S. and D. Rivin, *Solvent transport in hydrocarbon and perfluorocarbon ionomers.* Polymer, 2006. **47**(9): p. 3119-3131.
55. Baker, J., J. Comput. Chem., 1986. **7**: p. 385.
56. PQS, I., *PQS Ab Initio Program Package v 3.3*. 2004, Parallel Quantum Solutions: Fayetteville, Ark.
57. Suenram, R.D., et al., *Fourier transform microwave spectrum and ab initio study of dimethyl methylphosphonate.* Journal of Molecular Spectroscopy, 2002. **211**(1): p. 110-118.
58. Weinhold, F., *Natural Bond Orbital Analysis Program*. 2001, Univerity of Wisconsin: Madison WI.
59. Clark, M., R.D. Cramer, and N. vanOpdenbosch, *Validation Of The General-Purpose Tripos 5.2 Force-Field* Journal Of Computational Chemistry, 1989. **10**: p. 982.
60. Perera, L. and M.L. Berkowitz, *Ion Solvation in Water Clusters* Zeitschrift Fur Physik D-Atoms Molecules And Clusters, 1993. **26**: p. 166.
61. Gordon, P.A., *Development of intermolecular potentials for predicting transport properties of hydrocarbons.* Journal of Chemical Physics, 2006. **125**(1).
62. Harmandaris, V.A., et al., *Hierarchical modeling of polystyrene: From atomistic to coarse-grained simulations.* Macromolecules, 2006. **39**(19): p. 6708-6719.
63. Wick, C.D., M.G. Martin, and J.I. Siepmann, *Transferable potentials for phase equilibria. 4. United-atom description of linear and branched alkenes and alkylbenzenes.* Journal of Physical Chemistry B, 2000. **104**(33): p. 8008-8016.
64. Accelrys, I., *Cerius2*. 2000, Accelrys Inc: San Diego, CA.
65. Nose, S., *A Molecular-Dynamics Method for Simulations in the Canonical Ensemble.* Molecular Physics, 1984. **52**(2): p. 255-268.
66. Hoover, W.G., *Canonical Dynamics - Equilibrium Phase-Space Distributions.* Physical Review A 1985. **31**(3): p. 1695-1697.
67. Tuckerman, M., *Reversible multiple time scale MD.* Journal of Chemical Physics, 1992. **97**: p. 1990.
68. Lyubartsev, A.P. and A. Laaksonen, *M.DynaMix - a scalable portable parallel MD simulation package for arbitrary molecular mixtures.* Computer Physics Communications, 2000. **128**(3): p. 565-589.
69. Lyubartsev, A., *MDynaMix: a Molecular Dynamics Program*. 2007, Stockholm University: Stockholm.
70. Laaksonen, L., *gOpenMol*. 2001, CRC, Finnish IT centre for science: Espoo, Finland.
71. Vangunsteren, W.F. and H.J.C. Berendsen, *Algorithms for Macromolecular Dynamics and Constraint Dynamics.* Molecular Physics, 1977. **34**(5): p. 1311-1327.
72. Heinzinger, K., *Computer-Simulations of Aqueous-Electrolyte Solutions.* Physica B & C, 1985. **131**(1-3): p. 196-216.

73. Marchand, S. and B. Roux, *Molecular Dynamics Study of Calbindin D9k in the Apo and Singly and Doubly Calcium-Loaded States.* Proteins: Structure, Function, and Genetics, 1998. **33**(2): p. 265–284.
74. Rappe, A.K., et al., *Uff, a Full Periodic-Table Force-Field for Molecular Mechanics and Molecular-Dynamics Simulations.* Journal of the American Chemical Society, 1992. **114**(25): p. 10024-10035.
75. Megyes, T., et al., *Ion pairing in aqueous calcium chloride solution: Molecular dynamics simulation and diffraction studies.* Journal of Molecular Liquids, 2006. **129**(1-2): p. 63-74.
76. Bakker, A., et al., *Interaction of aluminum(III) with water. An ab initio study.* International Journal of Quantum Chemistry, 1999. **75**(4-5): p. 659-669.
77. Berendsen, H.J.C., J.R. Grigera, and T.P. Straatsma, *The Missing Term in Effective Pair Potentials.* Journal of Physical Chemistry, 1987. **91**(24): p. 6269-6271.
78. Calzia, K.J., A. Forcum, and A.J. Lesser, *Comparing reinforcement strategies for epoxy networks using reactive and non-reactive fortifiers.* Journal of Applied Polymer Science, 2006. **102**(5): p. 4606-4615.
79. Zerda, A.S. and A.J. Lesser, *Organophosphorous additive for fortification, processibility, and flame retardance of epoxy resins.* Journal of Applied Polymer Science, 2002. **84**(2): p. 302-309.
80. Zerda, A.S. and A.J. Lesser, *Characteristics of antiplasticized thermosets: Effects of network architecture and additive chemistry on mechanical fortification.* Polymer Engineering and Science, 2004. **44**(11): p. 2125-2133.
81. Vishnyakov, A., et al., *Molecular dynamics simulation of the alpha-D-Manp-(1 -> 3)-beta-D-Glcp-OMe disaccharide in water and water DMSO solution.* Journal of the American Chemical Society, 1999. **121**(23): p. 5403-5412.
82. Kowalewski, J. and E. Kovacs, *O-17 And Deuteron Nmr Relaxation Study Of Dimethylsulfoxide Water Mixture.* Zeitschrift Fur Physikalische Chemie Neue Folge 1986. **149**: p. 49.
83. Hoogerbrugge, P.J. and J. Koelman, *Simulating Microscopic Hydrodynamic Phenomena with Dissipative Particle Dynamics.* Europhysics Letters, 1992. **19**(3): p. 155-160.
84. Goujon, F., P. Malfreyt, and D.J. Tildesley, *Dissipative particle dynamics simulations in the grand canonical ensemble: Applications to polymer brushes.* ChemPhysChem, 2004. **4**: p. 457-464.
85. Won, J., et al., *Structural characterization and surface modification of sulfonated poly styrene-(ethylene-butylene)-styrene triblock proton exchange membranes.* Journal of Membrane Science, 2003. **214**(2): p. 245-257.